Journal of Hazardous Materials 474 (2024) 134747

Contents lists available at ScienceDirect

Journal of Hazardous Materials

journal homepage: www.elsevier.com/locate/jhazmat

The autoxidation of polyether-polyurethane open cell soft foam: An analytical aging method to reproducibly determine VOC emissions caused by thermo-oxidative degradation

Christian Stefan Sandten [a,*], Martin Kreyenschmidt [a], Rolf Albach [b]

[a] University of Applied Sciences Muenster, Hüfferstraße 27, 48149 Münster, Germany
[b] Covestro Deutschland AG, Kaiser-Wilhelm-Allee 60, 51373 Leverkusen, Germany

HIGHLIGHTS

- VOC formed by autoxidation in the absence of light.
- Autoxidative production rates of VOC are determined.
- Samples are purged of initial loading.
- Toxicological impact of polyurethane oxidation is discussed.

GRAPHICAL ABSTRACT

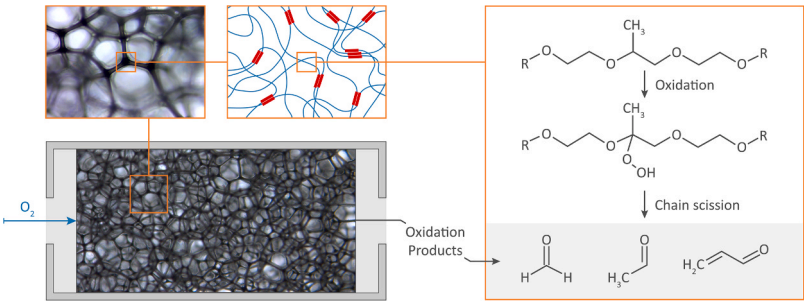

ARTICLE INFO

Keywords:
Formaldehyde
Acetaldehyde
Acrolein
Polyurethane
VOC
Autoxidation
VIAQ
NIAS
Toxicology
Flexible foam

ABSTRACT

We present a new method for investigating the oxidation and emission behavior of air-permeable materials. Employing this method, a differentiated statement can be made about the extent to which critical volatile organic compounds (VOCs) such as formaldehyde, acetaldehyde, and acrolein are contained in the material as impurities or formed by thermo-oxidative degradation of the polymer matrix in the use phase. The parameters affecting methods of VOC analysis are reviewed and considered for the developed method. The molecular mechanisms of VOC formation are discussed. Toxicological implications of the reaction kinetics are put into context with international guidelines and threshold levels. This new method enables manufacturers of cellular materials not only to determine the oxidative stability of their products but also to optimize them specifically for higher durability.

Environmental Implication: Cellular materials are ubiquitous in the technosphere. They play a crucial role in various microenvironments such as automotive interiors, building insulation, and cushioning. These materials are susceptible to oxidative breakdown, leading to the release of formaldehyde, acetaldehyde, and acrolein. The ecotoxicological profiles of these compounds necessitate monitoring and regulation. The absence of reproducible and reliable analytical methods restricts research and development aimed at risk assessment and mitigation. This work significantly enhances the toolbox for optimizing the oxidative stability of any open-cell cellular material and evaluating these materials in terms of their temperature-dependent oxidation and emission behavior.

* Corresponding author.
E-mail address: C.Sandten@FH-Muenster.de (C.S. Sandten).

https://doi.org/10.1016/j.jhazmat.2024.134747
Received 26 March 2024; Received in revised form 23 May 2024; Accepted 27 May 2024
Available online 28 May 2024
0304-3894/© 2024 The Authors. Published by Elsevier B.V. This is an open access article under the CC BY license (http://creativecommons.org/licenses/by/4.0/).

1. Introduction

1.1. Toxicology

Certain low molecular weight aldehydes, such as formaldehyde, acetaldehyde, and acrolein, pose toxicological risks to humans, leading to numerous investigations of their emissions [1–8]. Consequently, these aldehydes are regulated in a wide range of applications worldwide. According to Regulation (EC) No 1907/2006 Annex VI, the first two are classified as carcinogens and mutagens, acetaldehyde additionally as an eye irritant with specific target organ toxicity [9]. Formaldehyde and acrolein show acute toxicity, formaldehyde is skin corrosive and sensitizing.

1.2. Consumer protection

These three compounds, among others, are common contaminants in products derived from natural and fossil-based materials. They are introduced as synthesis byproducts or impure educts and are therefore labeled as non-intentionally added substances (NIAS). By contrast, formaldehyde can be introduced voluntarily as a component of the adhesive in materials such as particle boards. There is an abundance of contaminations embedded in polymer matrices, as the molecules themselves or as precursors, that may be emitted. Flexible, air-permeable polyurethane (PUR) foams are widely used in mattresses, upholstery, and automotive interiors [10]. For automotive applications, it has been shown that high temperatures strongly increase the emission of volatile organic compounds (VOC) [11–19]. Emissions are limited by a variety of factors, including diffusion coefficients, 'Henry' partition coefficients, and vapor pressure.

If these emission limiting factors were solely responsible for small aldehyde release, only transitory emissions would be observed due to relatively high diffusion coefficients, short diffusion lengths, and high vapor pressures. This is not the case. On the one hand, PUR foams continuously absorb and release VOC from and into the environment, starting from foam production over the assembly line up to the use phase. These uncontrolled variables are inherent to any analysis. On the other hand, organic compounds continuously form carbonyls like aldehydes upon oxidative stress. A comparative study showed that the concentration of formaldehyde, acetaldehyde, acetone, and acrolein in old vehicles decreased only by 6–11 % compared to new cars. In contrast, the concentrations of toluene, xylene, and ethylbenzene, which are NIAS and contaminations absorbed from the environment, were 51–55 %, lower in old compared to new cars [16].

In 2021 Zhu et al. analyzed 30 cars at ambient temperature and detected formaldehyde and acetaldehyde concentrations of 10–75 μg/m^3 and 28–103 μg/m^3 . Only at elevated temperatures acrolein became detectable with up to 26 μg/m^3 [20]. The interpretation of these values is challenging: the work only differentiates between room temperature and elevated temperature (ISO 12219–1-2012). The history of the investigated cars is not given. Therefore, the vehicle interior high temperature is defined by 4.5 h of external heat radiation into a vehicle with 400 ± 50 W/m^2. The material surface temperature and interior air temperature are not in equilibrium and both depend on the vehicle model, thermal insulation, and window material. Evidently, emissions relate rather to the material surface temperature than with the in-cabin air temperature. Material surface temperature changes are particularly pronounced on the dashboard rather than on the seat or the carpet where the majority of PUR is found [21].

The new EU REACH commission regulation sets a formaldehyde limit of 62 μg/m^3 for the interior of road vehicles [22]. This value is within the range of formaldehyde values found by Zhu. Therefore, there is a substantial need for targeted research into the optimization of vehicle interior materials to address this challenge.

1.3. Autoxidation in general

Aldehydes form when polymers oxidize [23–26] through a process called the basic autoxidation scheme (BAS) [27–33]. This occurs when hydrogen atoms are removed from the polymer chains, creating radicals. These radicals react with oxygen, forming peroxyl radicals. The peroxyl radicals then continue to extract hydrogen from the polymer, propagating the chain reaction and leading to further oxidation. Hydroperoxides can be stable up to 100 °C for several hours [34,35], but eventually cause molecular degradation and the formation of VOC. These processes are accelerated by light, elevated temperatures, and catalytically active metal ions like iron [27,36–41]. Weakly bonded hydrogens lead to a faster generation of radicals and the auto-acceleration of the autoxidation [42]. Accordingly, polymers exhibiting ether moieties, like polyether polyols used in PUR, are particularly susceptible to oxidative attack (Supplemental II: Figure 18, Figure 20, Figure 23) [43–57]. Surface temperatures of 85 °C have been measured on dashboards. Automotive industry tests range from accelerated aging at 120 °C for 21 days to 140 °C for seven days. Under such conditions, accelerated oxidative degradation of polymer foams can be expected [25,58,59]. Temperature-dependent formaldehyde levels within cars have been demonstrated over at least three years [18].

1.4. VOC-analysis and autoxidation of PUR

PUR soft foams are segmented elastomers comprising polyether soft segments and polyurea hard segments from the reactions of water with isocyanates, such as Methylene diphenyl diisocyanate (MDI) oligomers as used in this study. The polyethers are commonly copolymers or block-copolymers of poly ethylene-oxide (PEO) and poly propylene-oxide (PPO). For simplification, the majority of research focused on the degradation of the polyether soft segments of PUR and rarely on the entire material.

Qualitative and quantitative data on emissions from PUR foams at 23 °C are given in [60]. The authors identified various impurities introduced from raw materials. They show the initial loading of the investigated samples, and the analytes' diffusion and evaporation rates. Several studies investigated emissions and oxidation from PUR by Headspace-Gas chromatography-Mass spectrometry/Flame-Ionization-Detection (HS-GC-MS/FID) to characterize odorous components after natural and artificial aging [61] or to differentiate between the oxidative and hydrolytic durability of polyester and polyether-based PUR [62]. The impact of thermoplastic PUR formulations on acetaldehyde emission up to 130 °C has been investigated by HS-GC-FID. PPO containing PUR was the most susceptible substrate [59]. The aging of PUR has been investigated under air and nitrogen at 150 °C and under air, the formation of new VOCs has been reported within the foam [63]. Semi-volatile organic compounds (SVOC) from PUR raw materials, from PUR degradation, and byproducts of the PUR synthesis were observed between 70 °C and 300 °C using a series of collection traps [64].

Catalysts used for the polymerization of PUR commonly contain tertiary dimethylamino groups that can react with hydroperoxides to amine oxides. Degradation via Cope rearrangement can lead to formaldehyde and odorous amines [65–72].

1.4.1. Autoxidation of PUR hard segments

Hydroperoxide groups have been observed in the autoxidation of MDI, specifically on the methylene bridge between the two aromatic cores [73,74]. This has also been reported in the resulting carbamates within MDI-based PUR. These findings are significant because the oxidation of the hard-phase components can trigger the oxidation of the polyester soft segments [75–77].

1.4.2. Autoxidation of PUR soft segments

Polyether polyols are the typical soft segment in PUR flexible foam. The initial hydroperoxide concentration is linearly correlated to the

yellowing of the PUR [78].

In PUR, based on polyester polyol and aliphatic isocyanate, the thermal oxidation starts on the methylene groups adjacent to NH groups. Chemiluminescence experiments on a PUR foil in oxygen generated Arrhenius activation energies: up to 109 °C hydrolysis was the main degradation pathway. Between 109 °C and 202 °C chain oxidation becomes dominant, followed by direct chain scission above 202 °C [79].

The use of antioxidants decreases VOC emissions but the exact modes of action are unknown [80].

1.5. Autoxidation of polyethers

Polyethylene oxide (PEO) and Polypropylene oxide (PPO) blocks are the common constituents in the soft segment of segmented PUR in cars. The autoxidative stabilities of the homopolymers, copolymers, and block-copolymers has been investigated. PEO is less sensitive to oxidation than PPO [81,82]. At 25–40 °C PEO yields formaldehyde upon oxidation and PPO yields equimolar amounts of formaldehyde and acetaldehyde despite the difference in radical stability between secondary and primary CH next to the ether group [83]. Up to 80 °C PEO-PPO copolymers absorb oxygen and the hydroperoxide concentration increases linearly over time. At ~100 °C the concentration of hydroperoxides increases over 100 min and then drops to a quarter of the maximum. Hydroperoxide decomposition at 100 °C is approximately ten times faster than at 65 °C [35]. At 100 °C polyethers undergo statistical chain scission by the autocatalytic formation and decomposition of hydroperoxides rather than a chain end degradation [84,85]. For ethyl urethane end-capped PPO, the kinetic of oxygen absorption does not change between 110 °C and 140 °C compared to not end-capped PPO [86]. In an aprotic environment (o-dichlorobenzene) polyether oxidation rates are increased [35] while hydroxy groups inhibit autoxidation by the deactivation of peroxyl radicals via hydrogen bonding [27,40,82]. Various mechanisms for the oxidative breakdown of polyethers have been proposed and secondary alkoxy radicals seem to play an important role [87–89].

In the anionic polymerization of PO, a transfer reaction from the alcoholate to the PO monomer leads to allylate anions. These polymerize with PO to allyl-terminated polyether monools [90]. The low bond energy of the C-H bond of allyl ethers is particularly prone to autoxidation and the nature of the alkyl group in allyl-alkyl-ethers strongly impacts the autoxidation rates [39]. Allyl ethers serve as a suitable substrate to form acrolein by autoxidation (Supplemental II: Figure 26).

1.6. Analytical methods

Many analytical methods and derivatizing agents [91–99] qualify and quantify formaldehyde and other low molecular aldehydes [100–104]. The most common for the quantification of gaseous carbonyl functional compounds are adsorption-/derivatization-cartridges with Dinitrophenylhydrazine (DNPH) coated silica gel in tandem with High-Pressure-Liquid-Chromatography (HPLC) (see Fig. 1) [105–110].

Methods feature many parameters that can be varied, such as geometry, gas exchange rate, conditioning step, sample mass/geometry/surface area, sample and sampling device distance, and sampling temperature [111–115]. Several studies attempt to explain the varying formaldehyde emission results in different methods. These include parameters, such as relative humidity [116], sample chamber geometry [117], diffusion length from sample to sampling device [118], sample geometry [119], sample surface [115,120], time of measurement [121], laboratory personnel experience [122], temperature-dependent partition (K) and diffusion coefficient (D) and the initial loading (C_0) of a sample [123–132]. In the automotive industry, specific tests have been developed. Some are collected in the international standards ISO 12219 1–10 [133]. Others like the VDA275 are still in global use for the approval of materials by specific original equipment manufacturers (OEM) [113]. Some OEMs use pre-ISO-versions of testing methods to retain comparability to pre-ISO data. This is, for example, the case of the chamber tests GS97014–3 (BMW), PV3492 (VW), VDA276, and ISO 12219–4. All use 1 m^3 chambers at 65 °C/5 % humidity/0,4 AE h^{-1} but different conditioning procedures.

For PUR foams, the cellularity adds a challenge to VOC analysis [134,135]. The cell and polymer structure can lead to the retention of unknown amounts of VOC within the matrix. Urea groups or free amines chemisorb aldehydes by methylol or imine formation. PUR foams have high specific surface areas and are strongly adsorptive at low temperatures. This enables their application as a sampling medium for VOC [136–147]. The interpretation of VOC analysis results is further complicated by unknown cell structure, tortuosity, diffusion- and partition coefficients and the amount of surface and bulk material

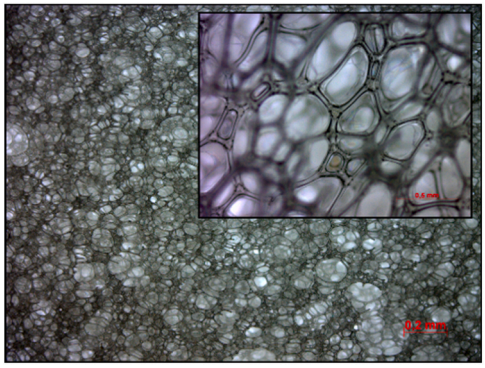

Fig. 2. Cell structure of investigated foam sample under microscope. Struts have an approximate diameter of 60 μm.

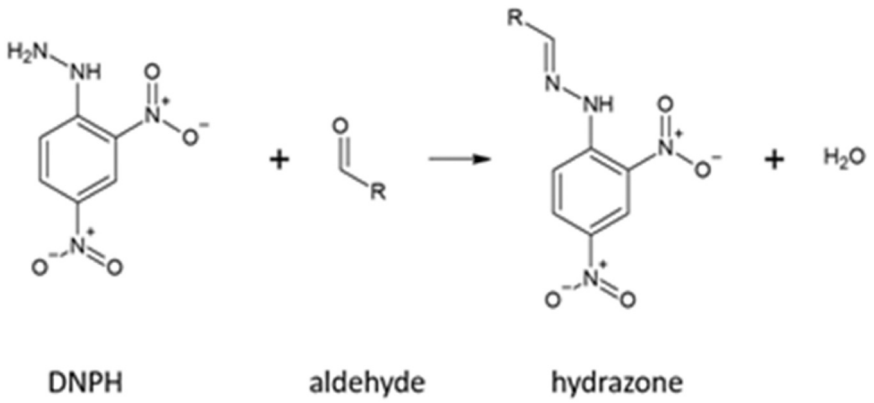

Fig. 1. Condensation reaction of DNPH with aldehydes, forming hydrazones and water.

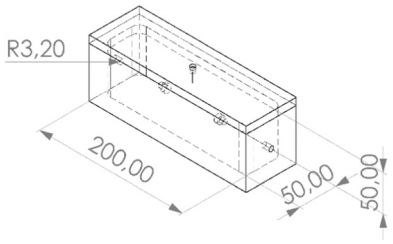

Fig. 3. Geometry of the developed sampling chamber. Annotated lengths in mm.

Fig. 4. Sample foam in sampling chamber.

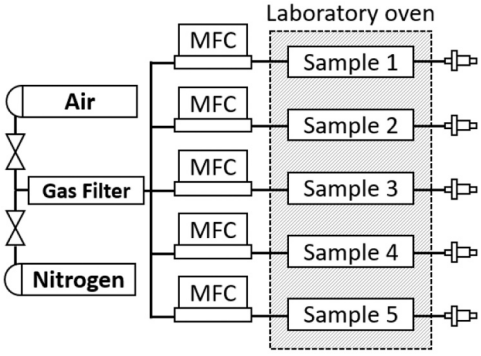

Fig. 5. Flow chart of sampling system.

influencing the measurement's results. These factors cannot be assessed or modelled yet.

1.7. Scientific gap

Most studies related to the thermo-oxidative degradation of PUR use TGA coupled with different analytical systems. These investigate the degradation up to temperatures of 1000 °C. They confirm that degradation in oxidative conditions occurs at lower temperatures than under nitrogen (30–70 K) [24,58,148–152]. In MDI-based PUR polyester- and polyether-based soft-segments differ in thermal stabilities. However, these experiments do not allow the evaluation of VOC emitted in realistic aging conditions [150].

Even though there are clear indications for oxidatively formed VOCs from PUR as part of VIAQ [16,18], currently, there is no method that quantifies oxidation products such as formaldehyde, acetaldehyde, or acrolein for a defined representative foam mass and volume in variable conditions. Furthermore, no method enables researchers to separately determine the oxidation rates and the amount of non-oxidatively formed

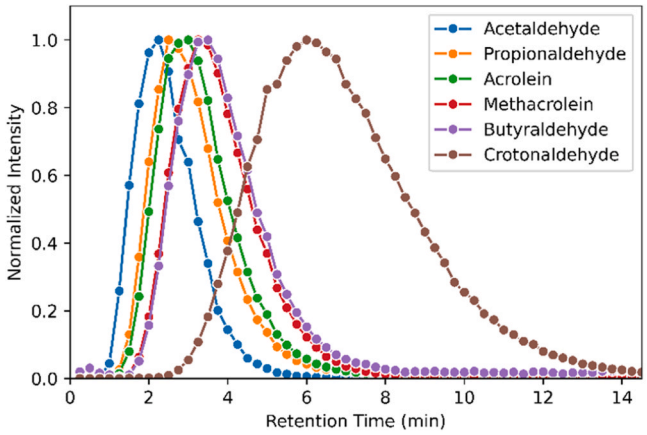

Fig. 6. Convective transport of analytes through sample (gas flow 200 mL/min). Acetaldehyde and acrolein were used as they are investigated in this work. Propionaldehyde, methacrolein, butyraldehyde and crotonaldehyde were used to investigate analytes with higher boiling points.

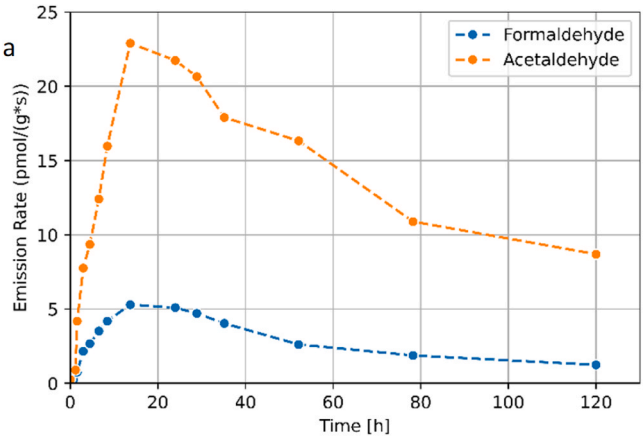

Fig. 7. Emission rate change over time for a polyurethane foam sample oxidized with air at 120 °C and flushed with 200 mL/min air (pre-purged for 24 h with 200 mL/min N2 at 120 °C). Emission rates were calculated as molar amount of formed hydrazone divided by sampling time and sample mass.

contaminations. Exclusively in this way, a differentiated root cause analysis of the VIAQ measurements would be possible.

The new method presented here allows for the first time to separately investigate the overlapping effects of oxidative degradation and initial loading of the material in an entire foam volume. The dimensions of the test specimen can be adapted to the analytical requirements. Test conditions such as temperature, gas composition, or humidity can selectively be adjusted. The atmospheric composition in the complete foam volume can easily be exchanged to investigate its influence on emissions. Steady-state autoxidation can be studied by quantifying the emission rates of aldehydes and other VOCs, and the toxicological relevance of autoxidative degradation of cellular materials can be assessed. Variation of the sampling duration allows an almost unrestricted limit of quantification (LOQ) for the emission rates of aldehydes.

2. Materials and methods

The setup for the foam sample conditioning and aging investigations consists of a PTFE chamber, a gas supply line with mass flow control, an oven for temperature control, a gas purification cartridge, and a sampling routine that allows time-dependent investigations. PTFE was chosen to lower the surface interaction of the chamber walls with analytes. The gas supply is used to continuously flush samples with purified

pressurized nitrogen or air. Other atmospheric conditions have been studied and will be reported elsewhere. The continuous renewal of the atmosphere within the foam leads to a shift of the adsorption equilibrium of VOCs into the gaseous phase. Removal of adsorbed analytes also lowers the surface concentration. This leads to an increase in analyte diffusion to the polymer surface. The chamber design and the cellularity of the sample lead to a plug flow with constant gas velocity throughout the sample's cross-section. This avoids back mixing of formed emittents within the sample. This improves sample flushing [153] and allows for the quick replacement of reactive atmosphere with inert gas [154]. The VOCs from the sample are convectively transferred outside the oven to DNPH-coated silica cartridges and analyzed by HPLC-DAD.

2.1. Chamber design and manufacture

A 70 mm by 70 mm by 220 mm PTFE block was milled to create a 50 mm by 50 mm by 200 mm cavity, resembling the shape of a sarcophagus. A second PTFE block was milled to create a fitting lid. The closed sampling chamber exhibits a ~500 mL cavity to hold foam samples of 50 mm by 50 mm by 200 mm.

A ¼-inch diameter hole was drilled into the two short ends of the chamber and a socket was fitted into each hole to allow the introduction of a sealing gasket made of a fluoroelastomer. Gas flow in and out of the chamber was established with ½-inch diameter PTFE tubing.

2.2. Foam synthesis

Foams were synthesized in a 16 L preheated (90 °C) mold. The synthesis mixture mass was calculated to be 650 g which led to negligible overpacking of the mold. Foams were synthesized with an index of 90 (100 *mol NCO/mol NCO-reactive groups). The isocyanate component was a blend of monomeric isomers of MDI and oligomeric homologs. The polyol was a blend of glycerol- and propylene glycol-started PPO-PEO-block-copolymers. The stirrer used for the foam synthesis was a Pendraulik LM 34. The synthesis mixture was stirred at 4200 rpm for 15 s and poured into the mold. The foam was de-molded after 45 min. The foam's density is 40.6 g/L.

2.3. Sample preparation

A serrated ceramic knife was used to cut off the outsides of the foam slab. Subsequently, the slab was cut into five pieces, roughly assuming a cuboid shape. Then a conventional household slicing machine, the Ritter Solida 4 was used to cut the required shape. Five foam samples were prepared as cuboids of 55 mm by 55 mm by 210 mm. Dimensions were chosen to be slightly wider than the chamber's inner volume to guarantee a gastight fit. The cuboids were taken from the center of the original sample and no foam skin was present on the finished sample cuboids.

Cuboids were fitted into the Teflon chambers and sealed from the outside with silicone and zip-ties.

2.4. Aging procedure

A laboratory oven, Binder Modell FD 115, was used for temperature control. Nitrogen was supplied by the university's nitrogen generator. Air was supplied by the university's air compressor. The samples were equilibrated at 120 °C in a constant air stream for 72 h before the investigations began. The temperature was chosen in accordance with VDA 278 to allow the simultaneous determination of VOC and SVOC.

2.5. Flow control

Flow control was established by using a Buerkert single-phase primary switched power supply, a CM22–0-10 V potentiometer by COBI ELECTRONIC, and Mass Flow Controllers type 8741 by Buerkert. The gas supplies were routed through an Agilent gas purifier cartridge, BIG HYDROCARBON TRAP Model BHT-4. Hydrocarbon levels are reduced to less than 15 ppb.

Teflon tubing was used to supply the sample chambers with gas flow and to direct emissions from inside the oven to the outside for sampling. Volume flow was set to 200 mL/min leading to a gas exchange rate of ~2.5 min^{-1}. The nitrogen supply was anhydrous, and the pressurized air's relative humidity at 19.7 °C at 8 % rH, equaling 1.15 g/kg or 1.48 g/m^3 . This equals 82.4 $mmol/m^3$ or 16 μmol/min or 274 nmol/s.

2.6. Sampling procedure

The sampling of the emissions took place by attaching a Sep-Pak DNPH-Silica Plus Short Cartridge with 350 mg sorbent (WAT037500) to the exhaust tubing. This way, the cartridge is located outside the oven at ambient temperature and remains at room temperature. The sampling duration was varied or chosen so that no saturation of the derivatizing agent could occur.

DNPH cartridges were eluted four hours after sampling with 5 mL of Acetonitrile into 5 mL ± 0.04 mL BLAUBRAND volumetric flasks and the flasks were filled up with Acetonitrile (LiChroSolv Reagent Grade).

2.7. HPLC

A VWR Elite LaChrom with an L-2300 column oven, L-2200 autosampler, L-2130 solvent pump, and L-2455 DAD detector was used for the analysis of hydrazone derivatives of emitted carbonyls. A 10 mm RP18e column guard and two Chromolith Performance RP18e 100 mm were used as analytical columns.

The solvents used were water, deionized by Sartorius arium pro, Acetonitrile LiChroSolv Reagent Grade, and Tetrahydrofuran HiPerSolv ChromaNorm (HPLC method in supplemental material I).

Restek Formaldehyde-2,4-DNPH Standard was purchased from VWR Los# A0160877.

Restek Acetaldehyde-2,4-DNPH Standard was purchased from VWR Los# A0165071.

To a solution of 2 g DNPH (pro analysi, Merck) phlegmatized with 0.5 mL water per gram in 40 mL Acetonitrile, 0.7 g analytical grade acrolein (purity 90 %, Sigma-Aldrich) containing hydroquinone and water was added. The precipitate was recrystallized twice from acetonitrile. The commercial formaldehyde-, acetaldehyde-, and the synthesized acrolein-derivative were used for external calibration.

The HPLC gradient program, external calibration, and peak area reproducibility data are found in supplemental material I and supplemental material III.

A blank value measurement of chambers not filled with foam was measured and no background values of formaldehyde, acetaldehyde, or acrolein were found.

3. Results

3.1. Convective analyte transport

The flow behavior of low molecular mass aldehydes through the foam sample was evaluated for plug flow. Acetaldehyde, propionaldehyde, acrolein, methacrolein, butyraldehyde, and crotonaldehyde were diluted in water to a concentration of 0.1 g/L. Propionaldehyde, methacrolein, butyraldehyde, and crotonaldehyde are not part of this research but are added to gain insight into the general adsorption-desorption behavior of aldehydes within the foam sample. In this experiment exclusively, formaldehyde was not investigated: the adsorption on thermodesorption tubes was not possible in sufficient amounts for GC-MS analysis.

The gas inlet of the sample chamber was fitted with a glass wool-filled three-way adapter to inject the aldehyde solution through a septum into the carrier gas stream. The gas outlet was fitted with a three-

way valve for continuous sampling of the emitted gas on Tenax TA thermodesorption tubes in 15-second intervals without loss of emitted gas or pressure pulses. The foam was purged with nitrogen at 120 °C for 24 h and 10 µL of the aldehyde solution was injected into the injection port. A timer was started simultaneously and a total of 58 samples were collected over 14.5 min. The samples were analyzed with a Shimadzu TD30R-GC-2030.

The analytes' retention times followed their boiling points. The free volume within the chamber minus the sample's volume is approximately 480 mL. The volume flow rate was 200 mL/min; therefore, the calculated dead time of the system is 2.4 min. The 10 µL liquid volume after evaporation is assumed to be ~17 mL, taking away from the system's dead volume and therefore 0.085 min of its dead time lowering it to 2.315 min

Assuming the acetaldehyde to elute from the foam without retention, at a retention time of 2.25 min, it travels 0.065 min faster than calculated (2.6 % of calculated dead time). This can be interpreted as 13 mL of the 500 mL of foam not directly participating in the analyte's chromatographic pathway.

The aldehydes show chromatographic interaction with the foam system: the analytes travel in approximate Gaussian distribution with some tailing through the sample. The tailing can be interpreted as a strong interaction of the analytes with the foam surface, some backmixing with the carrier gas, or a not instantaneous quantitative evaporation of the aqueous standard solution.

In general, all analyte curves drop back to their baseline level within a few minutes. Quantitative purging of VOC from the sample can be assumed.

3.2. Time-dependent oxidation/emission

In the first oxidation investigations, foams were purged for 24 h at 120 °C with a continuous flow of nitrogen. While the temperature was kept constant, the gas supply was changed from nitrogen to air. Following the general sampling procedure, a total of thirteen samples were taken over the course of a week with 15-minute sampling durations each. An immediate, rapid increase in emissions was observed over the first twelve hours. The emission rates at 120 °C increased to 5.29 pmol*$g^{-1}s^{-1}$ for formaldehyde and to 22.9 pmol*$g^{-1}s^{-1}$ for acetaldehyde.

Emission rates decreased over the next few days. A nearly steady state was observed after a week. Within 120 h, the emission rate of formaldehyde dropped to 23 % and acetaldehyde to 38 % of the respective peak rate. The rapid change in emissions did not allow evaluation of the reproducibility of the measurements. Therefore, it was assessed after the foam's emission rates reached a steady state. At this point, we investigated which sampling time would allow sufficient signal intensities and what the reproducibility of measurements was.

3.3. Determination of sampling time

The optimal sampling duration required to maximize analyte peak areas was investigated. DNPH cartridges were used to collect emissions from a sample with progressively extended sampling durations. The durations were 10 min, 15 min, 20 min, 30 min, 60 min, 120 min, 300 min, and 600 min (overlay of chromatograms in Fig. 8).

The peak areas increase linearly for all aldehyde derivatives within the first 300 min. After 300 min, the DNPH is nearly quantitatively consumed. After the DNPH is consumed, the amount of acetaldehyde drops below the 300-minute level. Formaldehyde and acrolein keep increasing linearly even though free DNPH is not available anymore (Fig. 9).

The total molar amount of consumed DNPH does not equal the sum of molar amounts of formaldehyde, acetaldehyde, and acrolein. Several other aldehydes and carbonyls are being emitted that react with DNPH (acetone, propionic aldehyde, methacrolein, benzaldehyde, 2-methylpentenal, and others).

The impact of the sampling duration was evaluated by single measurements. To give an estimation of the results' confidence interval, reference solutions with concentrations similar to those of the sample solutions were created, a tenfold measurement was conducted, and the expected error was calculated (alpha = 99, n = 10, Supplement I).

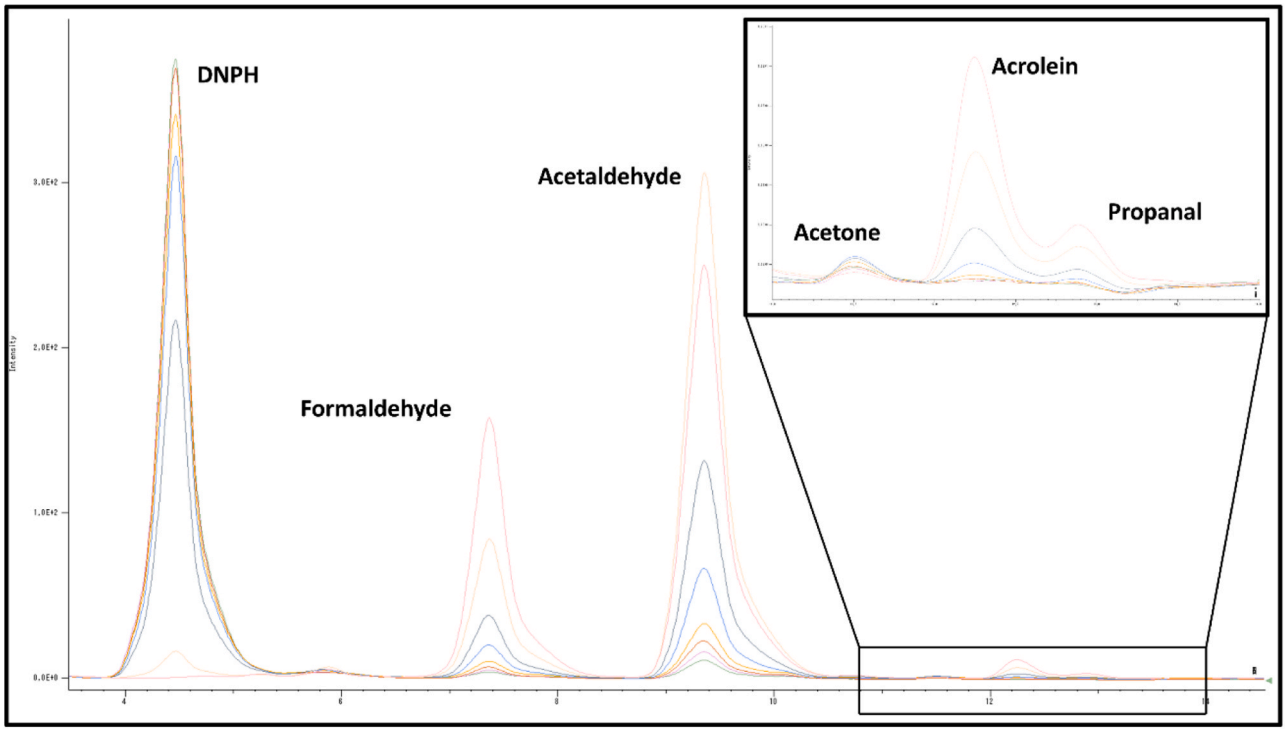

Fig. 8. Overlay of chromatograms measured for sampling duration optimization. Green: 10 min, Pink: 15 min, Red: 20 min, Yellow: 30 min, Blue: 60, Dark Blue: 120 min, Beige: 300 min, Magenta: 600 min.

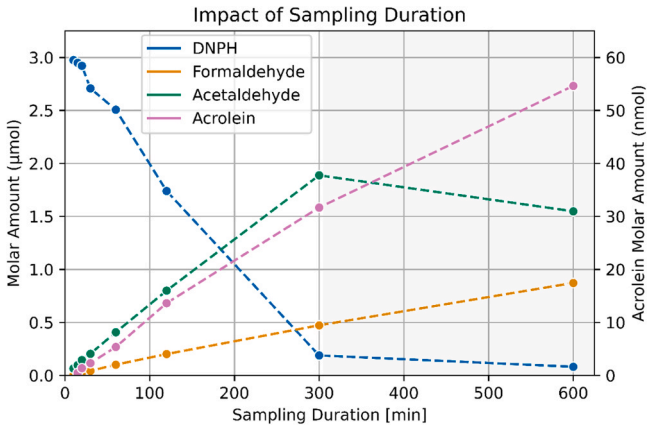

Fig. 9. Molar amount of analytes over sampling duration in minutes. The initial slopes within the first 300 min are 1,61 nmol/min for formaldehyde, 6.28 nmol/min for acetaldehyde, 0,11 nmol/min for acrolein, and − 9.75 nmol/min for DNPH. Assuming a first-order kinetics this corresponds to a rate of 10^{-5} min^{-1} for the reaction of acetaldehyde with formaldehyde. Quantitative sampling for acetaldehyde is not possible in the time range with a grey background.

The experiment shows two dedicated phases. Within the first phase, up to 300 min, there is free DNPH that is consumed by hydrazone formation as expected:

$$Ar\text{-}NH\text{-}NH_2 + R\text{-}CHO \rightarrow Ar\text{-}NH\text{-}N{=}CH\text{-}R + H_2O$$

$$(Ar = C_6H_3(NO_2)_3,\ R = H,\ CH_3,\ C_2H_3)$$

There is a second phase after 300 min marked by the absence of free DNPH. In this second phase, we find a decrease in acetaldehyde hydrazone content while the contents of the formaldehyde and acrolein hydrazones continue to increase. This could be explained by the displacement of acetaldehyde from the hydrazone on silica.

$$Ar\text{-}NH\text{-}N{=}CH\text{-}CH_3 + H\text{-}CHO \rightarrow Ar\text{-}NH\text{-}N{=}CH_2 + CH_3\text{-}CHO$$

As this assumption is based on a single measurement and has not been found in the literature yet, further investigations into trans-hydrazonification reactions are needed.

3.4. Determination of reproducibility

As 120 min sampling duration allowed quantitative analysis of all investigated aldehydes, five measurements on five foam samples were conducted to investigate the method's overall reproducibility (overlay of chromatograms in Fig. 10). The errors determined here encompass the inhomogeneity of the original foam slab the samples were cut from, the reproducibility of sample preparation (inter-sample comparability), the reproducibility of gas sampling, and the HPLC's system error (intra-sample reproducibility).

The sampling duration added up to over ten hours. Within this time interval, the measured peak areas showed no trend and remained approximately constant.

The relative standard deviations of the calculated emission rate of formaldehyde within the individual samples were 0.8 %, 0.4 %, 0.8 %, 1.3 %, and 1.3 % (intra-sample reproducibility). The standard deviation throughout all measurements and all samples was 6.1 % (inter-sample reproducibility).

For acetaldehyde, relative standard deviations of 1.7 %, 1.6 %, 1.3 %, 1.6 %, and 1.3 % were calculated. For all samples and measurements, a relative standard deviation of 6.7 % was determined.

The volumetric flasks have a volume of 5 mL ± 0,04 mL (0.8 %) and explain part of the peak area variance. The higher relative standard deviation across all measurements and all samples either reflects differences in the sample material, in the sample preparation, or both.

The relative standard deviations for acrolein were 7.3 %, 10.4 %, 6.81 %, 12.1 %, and 9.0 %. The overall relative standard deviation was 10.8 %. The comparatively high relative standard deviations of acrolein can be explained by its low emission rates and therefore low detected peak areas.

The confidence interval of formaldehyde emitted by all samples is calculated to be 1.22 pmol g^{-1} s^{-1} ± 0.04 (99 %, n = 25). The confidence interval of acetaldehyde emitted by all samples is 5.6 pmol g^{-1} s^{-1} ± 0.21 (99 %, n = 25) and of acrolein 106.9 fmol g^{-1} s^{-1} ± 6.4 (99 %,

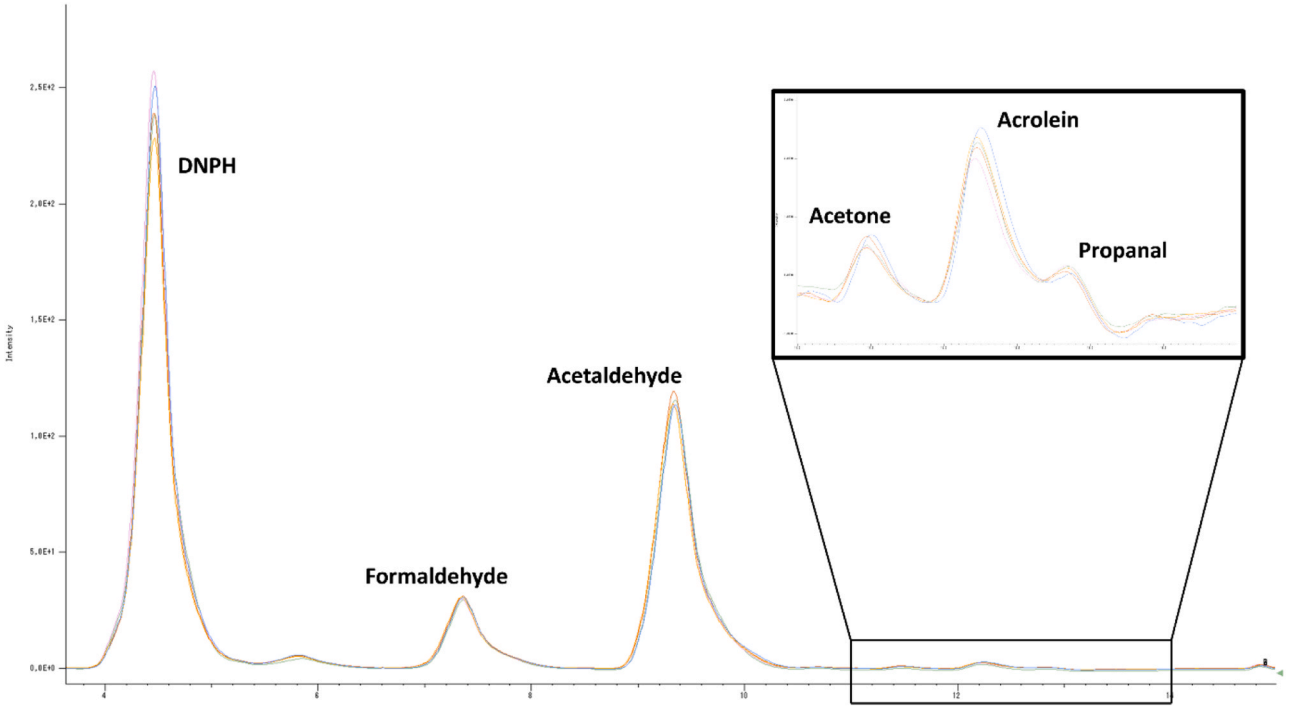

Fig. 10. Five repeated measurements of sample #1 over 120 min at 120 °C in a constant air stream at 200 mL/min.

n = 25) (see Fig. 11).

3.5. Impact of anaerobic conditions

To assess whether the observed emissions originate from an oxidative process, are compounds slowly diffusing through the foam's bulk material, or are being slowly desorbed, an experiment replacing air with nitrogen as reactant- and carrier gas was conducted.

Sample #1 used in the previous two experiments was conditioned at 120 °C in air and a sample was collected over 120 min. Subsequently, the gas supply was switched to nitrogen (120 °C) and five consecutive samples were collected over 120 min each. Afterward, the gas supply was switched back to air and another 2 h-sample was collected (Figs. 12, 13, 14). The initial emissions are below the values measured in the former two experiments as the sample was aged for over a week at this point and emissions slowly but continuously decreased over time as the polyether substrate in the matrix is consumed.

4. Discussion – interpretation

4.1. Convective analyte transport

The analytes travel in narrow bands through the sample. The retention times are in reasonably short ranges. The foam exhibits properties comparable to a chromatographic column. The majority of the sample volume participates in the pathway of the gaseous compounds. Back-mixing of analytes throughout the sample seems negligible.

4.2. Time-dependent emission

The oxidation of PUR open-cell foam follows the same basic autoxidation scheme as most other organic materials. The concentration of hydroperoxides increases continuously until a threshold level is met. There, the hydroperoxide rate of decomposition overtakes the one of formation. The emission rates then slowly decline over days. This trend can probably be accounted for by substrate consumption.

4.3. Sampling duration and hydrazone displacement hypothesis

The linear correlation of emitted mass over time demonstrates constant emission rates. After full consumption of free DNPH, acetaldehyde hydrazone seems to be displaced by formaldehyde and acrolein. At 300 min the emitted molar amount of acetaldehyde is 1.89 µmol ± 0.02 µmol and of formaldehyde 0.472 µmol ± 0.009 µmol. At 600 min the amount of formaldehyde increases by 0.400 µmol to 0.872 µmol ± 0.008 µmol, while the amount of acetaldehyde decreases by 0.339 µmol to 1.548 µmol ± 0.031 µmol. A transhydrazonification reaction could explain the observation. The 0.061 µmol difference can be explained by the 0.188 µmol ± 0.001 µmol DNPH left at 300 min dropping to 0.0815 µmol ± 0.0008 µmol and other hydrazones in addition to the acetaldehyde participating in the transhydrazonification.

This mechanism allows the accumulation of higher amounts of formaldehyde and acrolein as hydrazones but limits the measurable amount of acetaldehyde. This is not a problem in experiments where acetaldehyde is the main emission. However, in experiments targeting acetaldehyde, samples yielding predominantly formaldehyde, acrolein, or other more reactive carbonyl compounds might not accumulate sufficient acetaldehyde if DNPH is consumed before forming detectable amounts of acetaldehyde hydrazone. Despite concerns about long-term

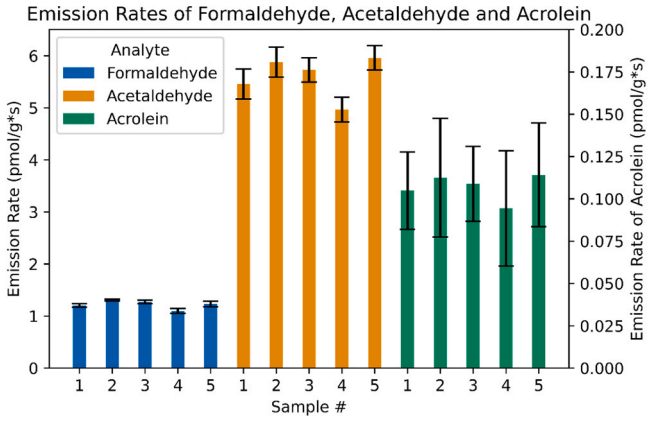

Fig. 11. Reproducibility of formaldehyde, acetaldehyde, and acrolein emissions. Five samples were measured five times. Results are given as averages and error bars represent three σ. Emissions are given in pmol/(g*s).

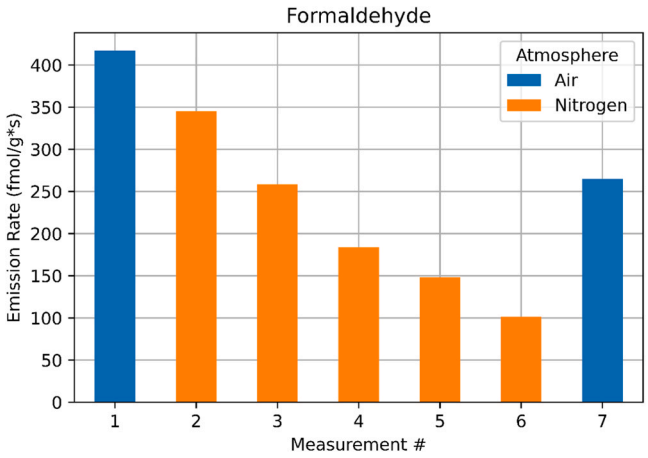

Fig. 12. Decline of formaldehyde emissions rates over time in anaerobic conditions at 120 °C in femtomole per gram and second. Each measurement (1–7) represents a time interval of 120 min. The foams had been under air flow (120 °C) for one week before making the first measurement. The oxidation does not reach the original oxidation rate again instantaneously after switching back to air, sample seven does not reach the original level. Further sampling (not shown here) leads to initial emission rates. The best fit is for a first-order kinetics ($\Delta c/\Delta t$) = 39,5 10^{-6} *t − 0677 (R^2 = 0992).

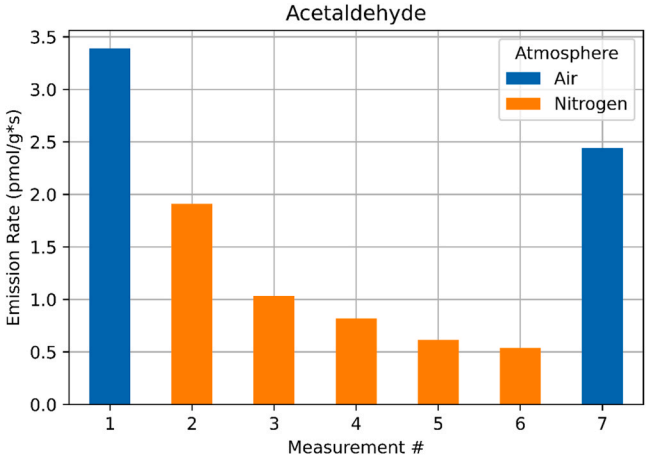

Fig. 13. Decline of acetaldehyde emissions over time in anaerobic conditions at 120 °C in picomole per gram and second. Each measurement (1–7) represents a time interval of 120 min. The foams had been under air flow (120 °C) for one week before making the first measurement. As the original oxidation rate is not immediately reached again after switching back to air, sample seven does not reach the original level. Further sampling (not shown here) leads to initial emission rates. The best fit is for a second-order kinetics $(\Delta c/\Delta t)^{-1}$ = 45,2 10^{-6} *t + 0,11 (R^2 = 0993).

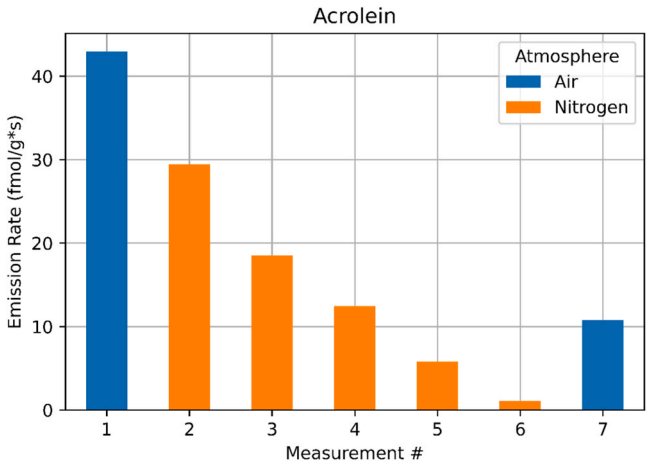

Fig. 14. Decline of acrolein emissions over time in anaerobic conditions at 120 °C in femtomole per gram and second. Each measurement (1–7) represents a time interval of 120 min. The foams had been under air flow (120 °C) for one week before making the first measurement. The oxidation does not instantaneously reach the original oxidation rate again after switching back to air. Thus, sample seven does not reach the original level. Further sampling (not shown here) leads to initial emission rates. The best fit is for first-order kinetics ($\Delta c/\Delta t$) = 67,6 10^{-6} *t + 4,08 (R^2 = 0,98).

sampling of formaldehyde, acetaldehyde, and acrolein, within the short two-hour timeframe tested here, no adverse effects on the quantification of these analytes were observed [155,156].

The confidence intervals for the reference solutions at the respectively closest concentration were applied to the sample solutions (Supplement III). The interpretation assumes the same sample-taking error for the 120-minute sampling duration as for different sampling durations.

4.4. Reproducibility

The relative standard deviations of repeated measurements within the samples are within the range of repeated HPLC measurements alone (Supplemental III). The gas sampling procedure and emission rate can be assumed to be constant and highly reproducible. The differences between the five sample foams are higher than within one sample foam. We assume that this can be accounted for by the hand-mixed foam's inhomogeneity rather than the errors in the sample preparation.

The constant emissions are interpreted as constant oxidation rates: Even if emissions were diffusion-limited, an equilibrium between analyte formation and analyte retention would be established.

Acrolein concentrations may be affected by dimerization and other side reactions in the foam, during transport, and on the silica cartridge [109,110,156,157]. We never found acrolein dimer in PUR foam using the VDA278 method for VOC and FOG. ASTM D5197–09 recommended eluting cartridges four hours after sampling to minimize the formation of derivatives and to generate the sum of the peak areas of acrolein and its derivatives. This procedure was retracted in D5197–21 as it does not account for unknown compounds, coelution, and differences in absorption coefficient [156,158–160]. Therefore, acrolein emission rates are subject to higher ambiguity and higher standard deviations can be explained with this factor as well.

4.5. Anaerobic conditions

Oxygen within the cells of the sample is replaced within approximately 2–3 min as back mixing can be neglected [154]. The slow decline in emissions over more than ten hours relates to a superimposition of a multitude of factors: the adsorption properties of substances, partition coefficients of analytes (K), diffusion rates of O_2 and the analytes (D) from and into the polymer, and the compound rates of the reactions leading to the formation of formaldehyde, acetaldehyde, and acrolein.

The slow decline of emissions after changing from aerobic to anaerobic conditions is in discordance with the high vapor pressure of the three analytes. Assuming an instantaneous transition of the oxidation products from the matrix to the gas phase (high D, low K), the sample's load should drop to near zero within minutes rather than hours. To approximate the time scale of formaldehyde diffusion, the foam struts' cross section was calculated assuming a uniform diameter of 60 µm to 28.3 * 10^{-6} cm^2. A homogenous concentration of oxygen throughout the strut was assumed. This leads to a constant oxidation rate throughout the whole polymer. There is evidence that at temperatures as high as 120 °C diffusion-limited oxidation (DLO) can occur and would lead to shorter diffusion lengths [161,162]. Hennebert listed formaldehyde diffusion coefficients through various polymers at 21, 40, and 60 °C [163]. Dividing the cross-section by the values given for amorphous polymers at 60 °C leads to approximated times in the order of 6–20 min. Extrapolating the listed values in an Arrhenius graph, diffusion of formaldehyde should take mere seconds to a few minutes due to the high diffusion coefficient and short diffusion pathway.

Partition coefficients between the surface and gas phase are highly vapor pressure- and temperature-dependent. As the atmosphere within the foam is continuously renewed, no equilibrium is achieved, and analytes are continuously removed from the polymer surface. Therefore, the impact of the partition coefficients should be negligible in our setup. The "stickiness" of the PUR matrix can be interpreted by chemisorption between small aldehydes and the urea hard segment (methylol formation) that could lead to diffusion- and partition-coefficients that differ significantly between phase-segregated PUR and other polymers. Our data supports the experience that in-silico models strongly overestimate the mass transfer rates from PUR to other media.

We assume the slow decline in emissions to reflect the slow degradation of hydroperoxides because neither the diffusion of analytes nor their partition coefficients influence the emission from the sample matrix. The differences in the declining rates could stem from the chemical diversity of hydroperoxide groups in the polymer. Comparable behavior has been reported for a decline in hydroperoxide concentration in polyether alcohol under nitrogen obeying first-order rate law at 100 °C [35]. It has been reported that hydroperoxides in thermoplastic PUR are fairly stable up to 90 °C and decompose readily within 15 h at 120 °C [34]. Our research is in good agreement with these time scales.

The decline of formaldehyde and acrolein follows first-order rate laws. This could be attributed to the degradation of hydroperoxides in the polyethylene oxide segment and the allylic ends of the polypropylene oxide being mostly unimolecular. Acetaldehyde emission follows an overall second-order rate law and could be attributed to the degradation of two adjacent hydroperoxides in the polypropylene oxide segment [41,164].

4.6. Organic chemistry

The foams used for this study are based on a blend of block-copolymers of PO and EO. The mass percentages of PO and EO are 86 % and 14 % respectively. This translates to molecular percentages of 82.3 % and 17.6 % and a PO/EO-ratio of 4.66 to 1.00. Kinetic selection leaves approx. 10 % of the initial PPO-block without a terminal PEO block and approx. 10 % of the terminal hydroxyl groups are secondary with significantly lower NCO-reactivity compared to the primary OH-groups of the PEO end blocks. The ratio of acetaldehyde emissions (5.60 pmol*g^{-1} *s^{-1} ± 0.21) to formaldehyde emissions (1.22 pmol/g*s ± 0.04) is 4.58 ± 0.33. While there are several mechanisms possible for PEO degradation that lead to formaldehyde (Supplemental II: Figure 18, Figure 19, Figure 27), PPO can lead to both acetaldehyde and formaldehyde (Supplemental II: Figure 21, Figure 22, Figure 24, Figure 25, Figure 28, Figure 29, Figure 30). Random scission conditions would yield a lower acetaldehyde-to-formaldehyde ratio than found.

There are at least two explanations for this. Firstly, the asymmetry of the polypropylene oxide could lead to selective oxidation to acetaldehyde. Mainly the oxidation of the tertiary carbon would occur and the hydroperoxide or peroxyl radical degrades (Supplemental II: Figure 28, Figure 29). No chain zipping mechanism would occur (Supplemental II: Figure 21, Figure 22, Figure 24, Figure 25). Secondly, based on the selectivity of the PUR reaction, at index 90 (10 % molar excess of NCO-reactive groups) only secondary hydroxyl end groups from PPO blocks are left after the polymerization. If those were favored in the oxidation reaction, the ratio of acetaldehyde to formaldehyde should be increased. Formates and acetates are also products of polyether oxidation and are also accessible by this method, when replacing DNPH cartridges with thermodesorption tubes. Their emission data shall eventually give insight into the degradation mechanisms.

Interestingly, while acrolein is, crotonaldehyde is not observed. The acetaldehyde concentration is much higher than the formaldehyde concentration. If one assumes that aldol condensation is responsible for acrolein formation, the question arises as to why crotonaldehyde is not observed. It is well known that PO rearranges to allyl alcohol under strongly alkaline conditions as found in anionic PO polymerization. This leads to some allyl-terminated polyether chains. We assume acrolein to be a primary oxidation product of these allyl ends rather than a secondary condensation product.

The decay curves in Figs. 12, 13, and 14 represent the compound kinetics of hydroperoxide decomposition to form aldehydes and diffusion to the surface of the polymer for convective transport to the sampling cartridge. Based on the limited stability of hydroperoxides at 120 °C we believe that its decomposition is the rate-determining step.

In the work of Hähner et al., hydroperoxide concentrations in polyether alcohols increased over ~120 min at 100 °C and then dropped to roughly a quarter of the maximal concentrations over the next ten hours [35]. We did not investigate hydroperoxide concentrations but products of hydroperoxide decomposition. Therefore, the highest emission rate would represent the highest hydroperoxide decomposition rate which should be slightly offset in time. Even though the temperature in this study was 20 K higher, the PUR polymer seems to respond slower to oxidation than the pure polyether alcohol investigated in the previous study. High viscosities in liquid polyethers have been identified as an oxidation reaction limiting factor. Thus it is not surprising that a solid material shows slower reaction rates even 170 °C above the glass transition temperature of the soft segment [82].

5. Implications

The new method is applicable to a wide range of cellular materials and potentially to fibrous materials such as textiles and carpets. To showcase the analytical method's potential to evaluate a material's impact on interior air quality, we used our data generated on polyurethane foams as an example. In addition to the data shown here, we measured emission rates at various temperatures to account for varying temperatures experienced in an automotive, which allowed us to investigate the relationship between temperature- and emission rate change.

We then applied acute concentration threshold values, such as odor limits and AEGLs to situations of acute exposure, like entering a heated car at 55 °C, and applied long-term concentration threshold values to regular usage conditions like driving in a car at 20 °C.

5.1. Scenarios

To put established toxicologically based limit values and the emission rates into perspective, a temperature-accelerated scenario in an automotive interior was estimated. The lifetime use of cars at ambient temperature with ventilation and the case of a car in a parking lot in the sun was taken into consideration. The maximum temperatures inside non-ventilated cars are well investigated because "pediatric deaths due to children being left in hot cars remain a significant yet preventable public health concern" [165]. After 60 min in the sun without ventilation, dashboard temperatures may reach 358 K (85 °C), and seat temperatures 328 K (55 °C). Typical automotive emissions tests like the normative ISO 12219–1 are at ambient temperatures that reflect the realistic scenario of long-term use of a car.

Further, a car with a zero-air exchange rate is assumed as in hyperthermia studies. For automobiles driving between 32–105 km/h, the air exchange rate ranges from 4 to 9 h^{-1} [166] and typical temperatures are at 290–295 K. Assuming a homogenous atmosphere and logarithmic decline of concentration over time this leads to a reduction of 86 % to 99 % of VOC concentration within the first 30 min [154]. Additionally, air exchange is going to lower the material temperatures reached.

The analytes are assumed to be quantitatively transferred from the cellular matrix to the vehicle's interior air although only in occupied seats is convective transport. The partition and diffusion coefficients from both the polymer matrix and the cellular material at various temperatures would be required to estimate the actual mass transfer. Additionally, restricted convection/diffusion caused by the foam's skin, cover, and cell structure are further limitations. A quantitative long-term transfer of analytes can be assumed if secondary reactions do not occur that consume the formed products.

Photooxidation, the effect of sunlight, is not taken into consideration. It affects only the uppermost layers of polymeric materials and polyurethane foams are usually covered by other materials.

This scenario does not account for initial hydroperoxide depots existing before the experiment nor accumulation of hydroperoxides and initially higher emission rates.

5.2. Concentration threshold values

5.2.1. Indoor air guide value – vehicle interior air quality for lifetime use

Indoor air guide levels (IAGL) of substances are derived from the German Committee on Indoor Air Guide Values (AIR) and consider lifetime exposure. Formaldehyde and acetaldehyde have IAGL I (precautionary guide values) of 100 $\mu g/m^3$. The IAGL II (hazard guide value) of acetaldehyde is 1000 $\mu g/m^3$ [167]. The EU-LCI (lowest concentration of interest) for formaldehyde is at 100 $\mu g/m^3$ and for acetaldehyde at 300 $\mu g/m^3$ [168].

This is represented in the current global standard for vehicle indoor air quality VIAQ ISO 12219–1 [133], the Chinese regulation GB/T 27630–2011 [169] (with currently the same threshold values as IAGL I for acetaldehyde and formaldehyde) and the Korean Automobile Management Act Article 33(3) [170].

EU Commission Regulation (EU) 2023/1464 of 14 July 2023 sets the threshold concentration of formaldehyde in the interior of vehicles to 62 $\mu g/m^3$ [22].

The US EPA derived a lifetime inhalation reference concentration for acrolein at 20 ng/m^3 [171].

5.2.2. Threshold values for acute effects

The calculations for acute exposure at 55 °C include low and high odor thresholds [172]. For formaldehyde, these are 1.47 mg/m^3 and 73.5 mg/m^3 , for acetaldehyde 0.2 mg/m^3 and 4.1 mg/m^3 and for acrolein 52.5 $\mu g/m^3$ and 37.5 mg/m^3 .

The 1 h US acute exposure guideline levels (AEGL) for formaldehyde, acetaldehyde and acrolein are AEGL-1 (discomfort); 1.1 mg/m^3 , 81 mg/m^3 and 70 $\mu g/m^3$, the AEGL-2 (disabling); 17 mg/m^3 , 490 mg/m^3 and 230 $\mu g/m^3$ and the AEGL-3 (lethal) values; 69 mg/m^3 , 1.5 g/m^3 and 3.2 mg/m^3 respectively [173–175].

5.3. Calculation

The lowest vehicle inner volume listed by Yoshida et al. [176] is 1.63 m^3 (mean volume was 3.74 m^3) and was used as the volume in this scenario. Further, 15 kg of foam is assumed as substrate mass although

not all foam is accessible e. g. due to cover materials.

The average formaldehyde emission rate in flow-through conditions at 120 °C of the five analyzed samples is 1.2 pmol*g^{-1} *s^{-1}. Calculating a mass-dependent mass emission rate gives a rate of 36.7 pg*g^{-1} *s^{-1}. Multiplied by 15 kg of foam, gives a mass emission rate of 550 ng/s. Assuming a car's volume of 1.63 m^3 a rate of 337.5 ng*s^{-1} *m^{-3} is calculated for the increase of formaldehyde concentration. Using the same boundaries gives rates of 2.26 µg*s * m^{-3} for acetaldehyde and 55.17 ng*s^{-1} *m^{-3} for acrolein.

The Arrhenius equation, expressed as $k = Ae^{-\frac{E_a}{RT}}$, where k is the reaction rate constant, A is the pre-exponential factor, E_a is the activation energy, R is the universal gas constant, and T is the temperature in Kelvin can be used to calculate temperature-dependent reaction rates when the values for A and E_a are known. In a separate experiment, temperature-dependent emission rates have been investigated between 65 °C and 155 °C in 15 K intervals, and the compound emission rates' activation energies were determined experimentally. Applying these of formaldehyde (~83 kJ/mole), acetaldehyde (~98 kJ/mole), and acrolein (~95 kJ/mole) to this study's emission rates, an approximation of temperature-dependent emission values can be made. These activation energies roughly equal a doubling to tripling of emission rates for every 10 K increase in temperature. They are comparable to the activation energy of the degradation of hydroperoxides in polyethers determined by Mikheyev [177]. A more detailed report about the kinetic of PUR oxidation and the linear part within the Arrhenius graph will be given in a future publication. The compound activation energies include the reactions leading to analyte formation, analyte desorption, and diffusion.

Using these activation energies, the material temperature-dependent emission rates can be calculated. With these calculated temperature-dependent emission rates, the time intervals in which threshold concentrations are reached can be approximated. They are plotted over the respective temperatures in Fig. 15, Fig. 16, and Fig. 17. These plots allow an assumption over the general worst-case time scale of the analytes' emission to reach critical levels. An exact calculation of emission rates is challenging as emission rates only stabilize long-term in a thoroughly oxidized sample (Fig. 7).

5.3.1. Acute exposure implications

The acute exposure values were compared to emission values extrapolated to 55 °C, a potential temperature faced when entering an unventilated parked vehicle. Chronic exposure thresholds were compared to the emission rates extrapolated to 20 °C, a common temperature at which an occupied vehicle is operated. Tables containing the calculated times are found in supplement IV.

For formaldehyde, no acute exposure thresholds are met within six days (1100 µg/m^3, US AEGL-1). For the case of acetaldehyde, the lower odor threshold (0.2 µg/m^3) is met within less than a minute. While not of toxicological concern, it seems reasonable to assume that acetaldehyde can be part of an automotive's interior air odor. For acetaldehyde concentrations to build up to uncomfortable US AEGL-1 (81000 µg/m^3), 157 days must pass. Acrolein needs three days to accumulate to a concentration noticeable by its odor (52.5 µg/m^3) and five days to reach its US AEGL-1 (70 µg/m^3).

Using the EPA interim acute exposure guideline levels AEGL and an Arrhenius extrapolation the emission rates calculated do not hint at a significant contribution of aldehydes to the hyperthermal stress in non-ventilated overheated cars.

5.3.2. Long-term exposure implications

Using the Arrhenius equation to extrapolate to 20 °C, the formaldehyde emission rate leads to the accumulation of 62 µg/m^3 (EU REACH) within 13 days and 100 µg/m^3 (EU-LCI, IAGL-I and GB/T 27630–2011) within 20 days in unventilated cars. The acetaldehyde thresholds of 100 µg/m^3 (IAGL-I and GB/T 27630–2011) and 300 µg/m^3 (EU-LCI) are met within 14 days and 42 days. Only the US lifetime reference concentration for acrolein is met within two hours.

Using available chronic exposure limit values, the detected and extrapolated emission rates of formaldehyde and acetaldehyde should not harm people in a car. The used emission data of convective mass

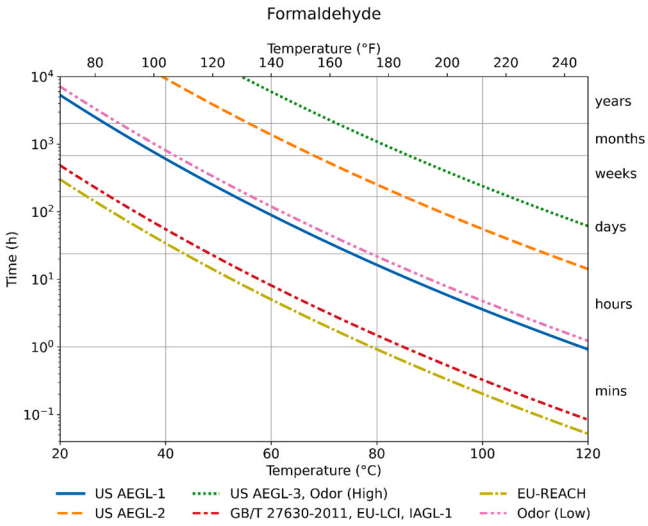

Fig. 15. Calculated temperature-dependent times for formaldehyde emissions to reach different threshold levels without ventilation, calculated in 1 K intervals. The ordinate is given in logarithmic scaling, the temperature both in Celsius and Fahrenheit. The horizontal grid is set to differentiate between minutes (1–60 min), hours (1–24 h), days (1–7 d), weeks (1–4 weeks), months (1–12 months) and years (1–10 a). AEGL-3 and the high odor threshold were combined in one line to optimize visibility: formaldehyde would not contribute to discomfort. US-AEGL-1 is on the low-odor threshold. The EU-LCI, IAGL-1, GB/T 27630–2011 are significantly below the odor range. EU-REACH for lifetime exposure is the lowest threshold level. These thresholds should not be reached in cars unventilated even for weeks.

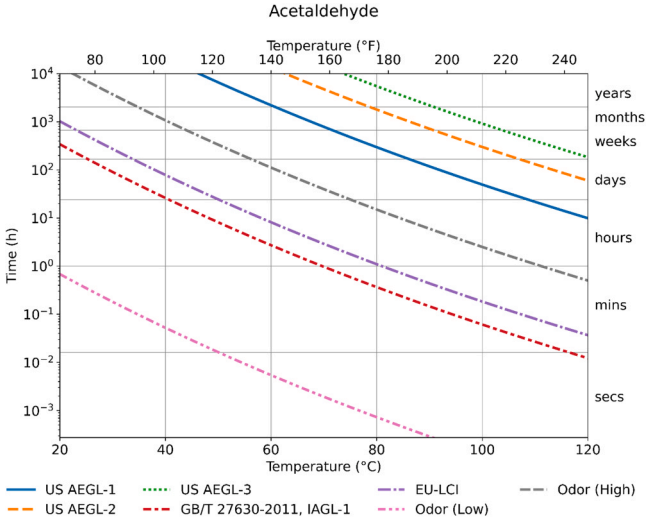

Fig. 16. Calculated temperature-dependent times for acetaldehyde emissions to reach different threshold levels without ventilation, calculated in 1 K intervals. The ordinate is given in logarithmic scaling, the temperature both in Celsius and Fahrenheit. The horizontal grid is set to differentiate between minutes (1–60 min), hours (1–24 h), days (1–7 d), weeks (1–4 weeks), months (1–12 months) and years (1–10 a). The US acute effect thresholds are all way above the high odor threshold. Lifetime acceptable thresholds are within the range detectable by the human nose: EU-CI, US AEGL-1, and Chinese thresholds are close to one another and would be reached in weeks in unventilated cars at ambient conditions. The low odor threshold is significantly below any toxicologically critical thresholds.

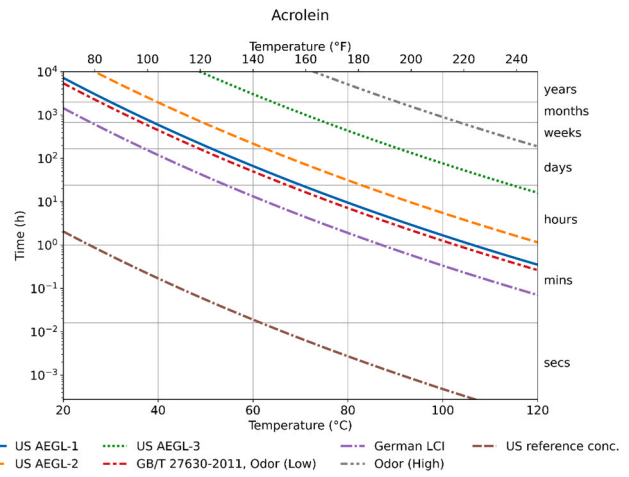

Fig. 17. Calculated temperature-dependent times for acrolein emissions to reach different threshold levels without ventilation, calculated in 1 K intervals. The ordinate is given in logarithmic scaling, the temperature both in Celsius and Fahrenheit. The horizontal grid is set to differentiate between minutes (1–60 min), hours (1–24 h), days (1–7 d), weeks (1–4 weeks), months (1–12 months) and years (1–10 a). GB/T 27630–2011 and the low odor threshold were combined to optimize visibility and the discomfort level US-AEGL-1 is very close. Most threshold levels are in the range between the high and the low odor threshold. The German lifetime LCI value is slightly below this level. These thresholds should not be reached in cars unventilated even for weeks. Only the US lifetime reference concentration is far below all other thresholds.

transport is assumed to represent a worst-case condition vs. the real use phase of a car. In a real car, analytes would form at elevated temperatures and be transported through the material by diffusion rather than convection. Our research does not account for time offsets between formation and emission. Within that time interval, the highly reactive compounds can participate in secondary reactions or be severely diluted by air exchange within the automobile.

Our research reflects VOC formation scenarios where hydroperoxide decomposition rates do not allow the build-up of significant hydroperoxide depots [178]. In a real-world scenario, hydroperoxides can form at lower temperatures and accumulate in the molecular backbone of the polymer. In case of a high-temperature event, the accumulated hydroperoxides' decomposition would accelerate, and VOC formation rates were higher than in an equilibrated system. Following such an event, proper ventilation is necessary to reduce the interior temperature and to mitigate the expected odor of acetaldehyde. This is a common practice for most individuals.

Air exchange rate, adsorption, lower temperatures, secondary reactions, foam tortuosity, restricted convection, and the amount of exposed material strongly limit the reaction rate and concentration build-up. Humidity shows a strong impact on the partition coefficient of formaldehyde and would therefore strongly impact its release into the vehicle's interior air volume [179]. Regular air exchange rates alone would keep aldehyde concentrations far below any critical levels for vehicle occupants.

The calculated times can be found in supplemental IV.

6. Summary

The new test method allows the investigation of the continuous and pseudo-steady state autoxidation from the sample matrix through the emitted VOC under variably selectable aging conditions. Formaldehyde, acetaldehyde, and acrolein from foam samples are reproducibly quantified. Steady-state oxidation, leading to constant analyte emissions, allows variable sampling times to adjust analyte emission mass to the analytical setup, and oxidation rates are accessible. With this unique setup, a broad range of emission rates is accessible due to the variability of sampling duration.

The method allows the investigation of the initial (anaerobic) emission of residues in foam from manufacturing and, after switching to aerobic conditions the investigation of various aging conditions. The impact of the open cell foam composition depending on humidity, acidity/basicity, and oxygen content on VOCs is accessible. Additionally, the impact of ozone or NO_x concentration on the oxidation rates and product spectrum is accessible with this method. Polyurethanes are in general quite stable against ozone due to a low amount of C═C double bonds in the polymer's backbone, however, unsaturated compounds like acrolein could be further degraded to smaller aldehydes.

The oxidation and emission rates reported here are interesting concerning the foam's decomposition pattern at elevated temperatures. PUR oxidation leads to formaldehyde, acetaldehyde, and acrolein but in regular automotive environments, critical concentrations are not expected. We report research using a bottom-up approach that (purposefully) does not reflect the impact of superimposed parameters (light, humidity, ozone, NO_x, mechanical stress, adsorption, diffusion) that can lead to increased or decreased emissions and is the subject of ongoing research. This research focuses on one exclusive but decisive parameter of the complex physical and chemical processes occurring in a car that is critical for a polymer's resistance to breakdown and its longevity.

The method is a powerful tool to investigate the decomposition mechanisms of any air-permeable polymer materials. The ratio of acetaldehyde to formaldehyde emissions at 120 °C may in the case of PUR reflect the polyethylene oxide to polypropylene oxide molar ratio within the polymer sample. A potential causal correlation is indicated and should be evaluated further using a broader variety of foam recipes. Assuming a random-chain-scission event, every emitted molecule would stand for at least one chain-scission event, lowering the material's degree of polymerization. This method gives a new perspective on the loss of degree of polymerization, average molecular mass, and crosslink density.

Over 10 h at 120 °C the formaldehyde emission rate drops to 25 %, acetaldehyde to 16 %, and acrolein to 2.6 %. The interpretation of VOC quantification results from short-term aging investigations, as oxidatively formed species, must be questioned. Acrolein formation may be more likely related to allyl end group oxidation than to aldol condensation. Short-term investigations cannot quantitatively stand for the actual quantity of aldehydes adsorbed/absorbed and formed.

When evaluating whether the oxidation and emission rates are relevant with regards to indoor air guide values, odor threshold, and toxicological thresholds, it becomes evident that PUR oxidation can play a factor in the long-term exposition of vehicle occupants to formaldehyde, acetaldehyde, and acrolein when ventilation is lacking. The toxicological and olfactorical interpretation will need more data on temperature dependencies, other VOCs, and the effect of ventilation behavior. Further results investigating temperature dependencies and other VOCs will be presented in further publications.

This method allows temperature-dependent emission analysis of a wide range of analytes when the sampling technique is adapted. As real-life samples are synthesized with a variety of additional additives and stabilizers a complex mixture of (semi-)volatiles is present. These VOC and SVOC are accessible using thermo-desorption tubes in tandem with TD-GC-MS and will be published in the future.

The toxicological interpretation omits those parameters that typically prohibit the determination of oxidation rates from VOC analysis. This means that air exchange rates, adsorptive effects, partition, and diffusion coefficients, which would strongly limit the release of VOC into the atmosphere, are not accounted for. Further, the temperature of our investigation stands for an extreme temperature that even a vehicle dashboard can't reach and is very unlikely to occur in the bulk of the material – except in standard automotive accelerated aging tests. Therefore, the PUR samples investigated are expected to be toxicologically safe in real-world applications. However, other PUR samples or materials more prone to oxidation could be investigated in shorter time

frames or lower temperatures according to their emission profile to investigate their toxicological profile.

With increasing legislative pressure on polymer manufacturers, targeted emission research becomes essential. The EUROPUR association states that "flexible PUR foam should never exceed the emission limits for general articles" while the new threshold for cars "could potentially require changes in formulations and modifications of plant infrastructure" [180]. This new method is a powerful tool for the research and development of materials that are more durable towards thermo-oxidative stress with lower initial loadings. Further, the long-term emission profiles of materials can be investigated.

Funding

This work was supported by the Covestro Deutschland AG. Leverkusen.

CRediT authorship contribution statement

Martin Kreyenschmidt: Writing – review & editing, Writing – original draft, Supervision, Project administration, Funding acquisition. **Christian Stefan Sandten:** Writing – review & editing, Writing – original draft, Visualization, Validation, Methodology, Investigation, Formal analysis, Data curation, Conceptualization. **Rolf Albach:** Writing – review & editing, Writing – original draft, Supervision.

Declaration of Competing Interest

The authors declare the following financial interests/personal relationships which may be considered as potential competing interests: Christian Sandten reports financial support was provided by Covestro AG. Dr. Rolf Albach reports a relationship with Covestro AG that includes: employment. Christian Sandten reports a relationship with FH Münster University of Applied Sciences - Steinfurt Campus that includes: employment. Dr. Martin Kreyenschmidt reports a relationship with FH Münster University of Applied Sciences - Steinfurt Campus that includes: employment. If there are other authors, they declare that they have no known competing financial interests or personal relationships that could have appeared to influence the work reported in this paper.

Data availability

Data will be made available on request.

Acknowledgments

Academic discussion and guidance: Torsten Hagen, Swantje Lersch, Hans-Georg Pirkl, Guidance for toxicological evaluation: Prof. Dr. Schupp, Guidance for statistical analysis: Prof. Dr. Schlitter, Guidance for data visualization: Michael Breuckmann, Proofreading: Sierra Pitman, Stephanie Hanning, Translation of literature: Illia Rudenko, Anastasia Vinogradova, Graphical abstract design: Rachel Jorgensen.

Appendix A. Supporting information

Supplementary data associated with this article can be found in the online version at doi:10.1016/j.jhazmat.2024.134747.

References

[1] Merk, O., Speit, G., 1998. Significance of formaldehyde-induced DNA–protein crosslinks for mutagenesis. Environ Mol Mutagen 32, 260–268.
[2] Coggon, D., Harris, E.C., Poole, J., Palmer, K.T., 2003. Extended follow-up of a cohort of british chemical workers exposed to formaldehyde. Cancer Knowl Environ 95, 1608–1615.
[3] Baua, Begründung zu Acrylaldehyd in TRGS 900: Acrylaldehyde (Acrolein, 2-Propenal), 2006.
[4] Institut für Arbeitsschutz der Deutschen Gesetzlichen Unfallversicherung (Ed.), Liste der krebserzeugenden, keimzellmutagenen und reproduktionstoxischen Stoffe (KMR-Stoffe), 2022.
[5] Ifa, Formaldehyd, 2023.
[6] Institut für Arbeitsschutz der Deutschen Gesetzlichen Unfallversicherung, Acetaldehyd, 2023.
[7] Institut für Arbeitsschutz der Deutschen Gesetzlichen Unfallversicherung, Acrolein, 2023.
[8] Acrolein [MAK Value Documentation, 2001], in: Deutsche Forschungsgemeinschaft (Ed.), The MAK-collection for Occupational Health andSafety: Annual Thresholds and Classifications for the Workplace: Grenzwerte in biologischem Material, 28.01.2014, pp. 1–33.
[9] Echa, Annex VI to CLP_ATP18, 2023.
[10] Engels, H.-W., Pirkl, H.-G., Albers, R., Albach, R.W., Krause, J., Hoffmann, A., Casselmann, H., Dormish, J., 2013. Polyurethanes: versatile materials and sustainable problem solvers for today's challenges. Angew Chem 52, 9422–9441.
[11] Buters, J.T.M., Schober, W., Gutermuth, J., Jakob, T., Aguilar-Pimentel, A., Huss-Marp, J., Traidl-Hoffmann, C., Mair, S., Mair, S., Mayer, F., Breuer, K., Behrendt, H., 2007. Toxicity of parked motor vehicle indoor air. Environ Sci Technol 41, 2622–2629.
[12] Chan, C.-C., Spengler, J.D., Özkaynak, H., Lefkopoulou, M., 1991. Commuter exposures to VOCs in Boston, Massachusetts. J Air Waste Manag Assoc 41, 1594–1600.
[13] Chen, X., Feng, L., Luo, H., Cheng, H., 2014. Analyses on influencing factors of airborne VOCS pollution in taxi cabins. Environ Sci Pollut Res 21, 12868–12882.
[14] Chien, Y.-C., 2007. Variations in amounts and potential sources of volatile organic chemicals in new cars. Sci Total Environ 382, 228–239.
[15] Xiong, J., Yang, T., Tan, J., Li, L., Ge, Y.-S., 2015. Characterization of VOC emission from materials in vehicular environment at varied temperatures: correlation development and validation. PLOS ONE 10, e0140081.
[16] Xu, B., Wu, Y., Gong, Y., Wu, S., Wu, X., Zhu, S., Liu, T., 2016. Investigation of volatile organic compounds exposure inside vehicle cabins in China. Atmos Pollut Res 7, 215–220.
[17] Guo, R., Zhu, X., Zhu, Z., Sun, J., Li, Y., Hu, W., Tang, S., 2022. Evaluation of typical volatile organic compounds levels in new vehicles under static and driving conditions. Int J Environ Res Public Health 19.
[18] Yoshida, T., Matsunaga, I., 2006. A case study on identification of airborne organic compounds and time courses of their concentrations in the cabin of a new car for private use. Environ Int 32, 58–79.
[19] Kerkeling, S., Sandten, C., Schupp, T., Kreyenschmidt, M., 2021. VOC emissions from particle filtering half masks - methods, risks and need for further action. EXCLI J 20, 995–1008.
[20] Zhu, Z., Liu, X., Xu, S., 2021. Research on the interior air quality and pollution control in new vehicles in China. IOP Conf Ser: Earth Environ Sci 804, 42080.
[21] Wang, H., Guo, D., Zhang, W., Zhang, R., Gao, Y., Zhang, X., Liu, W., Wu, W., Sun, L., Yu, X., Zhao, J., Xiong, J., Huang, S., Wolfson, J.M., Koutrakis, P., 2023. Observation, prediction, and risk assessment of volatile organic compounds in a vehicle cabin environment. Cell Rep Phys Sci 4, 101375.
[22] Publications Office of the European Union, L-2985 Luxembourg, Commission Regulation (EU) 2023/1464 of 14 July 2023 amending Annex XVII to Regulation (EC) No 1907/2006 of the European Parliament and of the Council as regards formaldehyde and formaldehyde releasers: (Text with EEA relevance), Official Journal of the European Union 2023 L 180/12-L 180/20.
[23] Allan, D., Daly, J.H., Liggat, J.J., 2013. Thermal volatilisation analysis of TDI-based flexible polyurethane foam. Polym Degrad Stab 98, 535–541.
[24] Rosu, D., Tudorachi, N., Rosu, L., 2010. Investigations on the thermal stability of a MDI based polyurethane elastomer. J Anal Appl Pyrolysis 89, 152–158.
[25] Grassie, N., Perdomo Mendoza, G.A., 1984. Thermal degradation of polyether-urethanes: Part 1—Thermal degradation of poly(ethylene glycols) used in the preparation of polyurethanes. Polym Degrad Stab 9, 155–165.
[26] Grassie, N., Zulfiqar, M., Guy, M.I., 1980. Thermal degradation of a series of polyester polyurethanes. J Polym Sci Polym Chem Ed 18, 265–274.
[27] S.S. Stahl, P.L. Alsters, Liquid Phase Aerobic Oxidation Catalysis: Industrial Applications and Academic Perspectives, Wiley-VCH Verlag GmbH & Co. KGaA, Weinheim, Germany, 2016.
[28] Smith, L.M., Aitken, H.M., Coote, M.L., 2018. The fate of the peroxyl radical in autoxidation: how does polymer degradation really occur? Acc Chem Res 51, 2006–2013.
[29] Gillen, K.T., Wise, J., Clough, R.L., 1995. General solution for the basic autoxidation scheme. Polym Degrad Stab 47, 149–161.
[30] Bolland, J.L., 1946. Kinetic studies in the chemistry of rubber and related materials. I. The thermal oxidation of ethyl linoleate. Proc R Soc Lond A 186, 218–236.
[31] Bolland, J.L., Gee, G., 1946. Kinetic studies in the chemistry of rubber and related materials. II. The kinetics of oxidation of unconjugated olefins. Trans Faraday Soc 42, 236.
[32] Bolland, J.L., Gee, G., 1946. Kinetic studies in the chemistry of rubber and related materials. III. Thermochemistry and mechanisms of olefin oxidation. Trans Faraday Soc 42, 244.
[33] Bateman, L., 1954. Olefin oxidation. Q Rev, Chem Soc 8, 147.
[34] Lemaire, J., Arnaud, R., Gardette, J.-L., 1983. The role of hydroperoxides in photooxidation of polyolefins, polyamides and polyurethane elastomers. Pure Appl Chem 55, 1603–1614.
[35] Hähner, U., Habicher, W.D., Schwetlick, K., 1991. Studies on the thermooxidation of ethers and polyethers: Part I—The uninhibited thermooxidation of a polyether. Polym Degrad Stab 34, 111–118.

[36] Bäckström, H.L.J., 1927. The chain-reaction theory of negative catalysis. J Am Chem Soc 49, 1460–1472.
[37] Carlsson, D.J., Wiles, D.M., 1969. The photodegradation of polypropylene films. III. Photolysis of polypropylene hydroperoxides. Macromolecules 2, 597–606.
[38] Neuenschwander, U., Hermans, I., 2012. Thermal and catalytic formation of radicals during autoxidation. J Catal 287, 1–4.
[39] Toivonen, H., Ahlberg, P., Rømming, C., Sköldefors, H., Wilking, N., Theve, N.O., 1984. Autoxidation of allyl ether compounds. Part II. Reactivity of alkyl allyl ethers. Acta Chem Scand 38b, 63–66.
[40] Toivonen, H., Lajunen, L.H.J., Holster, T., Hietaniemi, L., Nupponen, H., Theve, N.O., 1984. Autoxidation of allyl ether compounds. Part 1. Reactivity of allyl ether alcohols. Acta Chem Scand 38b, 37–42.
[41] Thomassin, C., Marchal, J., 1977. Réactions primaires de dégradation oxydante au cours de l'autoxydation du poly(oxytétraméthylène) à 25°C, 1. Caractérisation de la production d'éthylène. Die Makromol Chem 178, 981–1003.
[42] Turrà, N., Neuenschwander, U., Hermans, I., 2013. Molecule-induced peroxide homolysis. Chemphyschem a Eur J Chem Phys Phys Chem 14, 1666–1669.
[43] Mortensen, M.N., Egsgaard, H., Hvilsted, S., Shashoua, Y., Glastrup, J., 2012. Tetraethylene glycol thermooxidation and the influence of certain compounds relevant to conserved archaeological wood. J Archaeol Sci 39, 3341–3348.
[44] Clover, A.M., 1922. The autoxidation of ethyl ether. J Am Chem Soc 44, 1107–1118.
[45] Clover, A.M., 1924. Auto-oxidation of ethers. J Am Chem Soc 46, 419–430.
[46] Stokes, K., Coury, A., Urbanski, P., 1987. Autooxidative degradation of implanted polyether polyurethane devices. J Biomater Appl 1, 411–448.
[47] Bai, S., Chen, K., Huang, W., Wang, P., Chen, X., Chen, P., 2023. Thermo-oxidative degradation of ultrahigh molecular weight poly(ethylene oxide) in volatile organic solvents. Polym Adv Technol. 34, 613–620.
[48] Costa, L., Camino, G., Luda, M.P., Cameron, G.G., Qureshi, M.Y., 1996. The thermal oxidation of poly(propylene oxide) and its complexes with LiBr and LiI. Polym Degrad Stab 53, 301–310.
[49] Costa, L., Gad, A.M., Camino, G., Cameron, G.G., Qureshi, M.Y., 1992. Thermal and thermooxidative degradation of poly(ethylene oxide)-metal salt complexes. Macromolecules 25, 5512–5518.
[50] Decker, C., Marchal, J., 1973. Caracterisation de reactions primaries de degradation oxydante au cours de l'autoxidation des polyoxyethylenes a 25 °C: etude en solution aqueuse avec amorcage par radiolyse du solvant: VI. Polyoxyethylene: produits d'oxydation et schema cinetique. Die Makromol Chem 166, 155–178.
[51] Dulog, V.L., Storck, G., 1966. Die Oxydation von Polyepoxiden mit molekularem Sauerstoff. Die Makromol Chem 91, 50–73.
[52] Rieche, A., 1958. Über Peroxyde der Äther, der Carbonyl-Verbindungen und die Ozonide. Angew Chem 70, 251–266.
[53] Rieche, A., Meister, R., 1936. Modellversuche zur Autoxydation der Äther. Angew Chem 49, 101–103.
[54] Gordon Cameron, G., Ingram, M.D., Younus Qureshi, M., Gearing, H.M., Costa, L., Camino, G., 1989. The thermal degradation of poly(ethylene oxide) and its complex with NaCNS. Eur Polym J 25, 779–784.
[55] Han, S., Kim, C., Kwon, D., 1995. Thermal degradation of poly(ethyleneglycol). Polym Degrad Stab 47, 203–208.
[56] Madorsicy, S.L., Straus, S., 1959. Thermal degradation of polyethylene oxide and polypropylene oxide. J Polym Sci 36, 183–194.
[57] Plucinski, J., Janik, R., 1982. Die thermooxidative Zersetzung nichtionogener Tenside vom Pluronic-Typ. Tenside Surfactants Deterg 19, 83–87.
[58] Allan, D., Daly, J.H., Liggat, J.J., 2019. Oxidative and non-oxidative degradation of a TDI-based polyurethane foam: Volatile product and condensed phase characterisation by FTIR and solid state 13C NMR spectroscopy. Polym Degrad Stab 161, 57–73.
[59] Choi, Y.J., Alagi, P., Jang, J.H., Lee, S.J., Yoon, Hy, Hong, S.C., 2018. Compositional elements of thermoplastic polyurethanes for reducing the generation of acetaldehyde during thermo-oxidative degradation. Polym Test 68, 279–286.
[60] Hillier, K., Schupp, T., Carney, I., 2003. An investigation into VOC emissions from polyurethane flexible foam mattresses. Cell Polym 22, 237–259.
[61] Thiébaut, B., Lattuati-Derieux, A., Hocevar, M., Vilmont, L.-B., 2007. Application of headspace SPME-GC-MS in characterisation of odorous volatile organic compounds emitted from magnetic tape coatings based on poly(urethane-ester) after natural and artificial ageing. Polym Test 26, 243–256.
[62] Lattuati-Derieux, A., Thao-Heu, S., Lavédrine, B., 2011. Assessment of the degradation of polyurethane foams after artificial and natural ageing by using pyrolysis-gas chromatography/mass spectrometry and headspace-solid phase microextraction-gas chromatography/mass spectrometry. J Chromatogr A 1218, 4498–4508.
[63] Yarahmadi, N., Vega, A., Jakubowicz, I., 2017. Accelerated ageing and degradation characteristics of rigid polyurethane foam. Polym Degrad Stab 138, 192–200.
[64] Watanabe, M., Nakata, C., Wu, W., Kawamoto, K., Noma, Y., 2007. Characterization of semi-volatile organic compounds emitted during heating of nitrogen-containing plastics at low temperature. Chemosphere 68, 2063–2072.
[65] B.N. Barman, R. Grigsby, INHIBITION OF AMINE OXIDATION - European Patent Office - EP 2521746 B1: EUROPEAN PATENT, 2010.
[66] Barman, B.N., 2014. Accurate determination of aldehydes in amine catalysts or amines by 2,4-dinitrophenylhydrazine derivatization. J Chromatogr A 1327, 19–26.
[67] Kok, G.B., Pye, C.C., Singer, R.D., Scammells, P.J., 2010. Two-step iron(0)-mediated N-demethylation of N-methyl alkaloids. J Org Chem 75, 4806–4811.
[68] Kok, G.B., Scammells, P.J., 2011. Efficient iron-catalyzed N-demethylation of tertiary amine-n-oxides under oxidative conditions. Aust J Chem 64, 1515.
[69] Mary, A., Renko, D.Z., Guillou, C., Thal, C., 1997. Selective N-demethylation of galanthamine to norgalanthamine via a non classical Polonovski reaction. Tetrahedron Lett 38, 5151–5152.
[70] McCamley, K., Ripper, J.A., Singer, R.D., Scammells, P.J., 2003. Efficient N-demethylation of opiate alkaloids using a modified nonclassical Polonovski reaction. J Org Chem 68, 9847–9850.
[71] Ruda, A.M., Papadouli, S., Thangavadivale, V., Moseley, J.D., 2022. Application of the polonovski reaction: scale-up of an efficient and environmentally benign opioid demethylation. Org Process Res Dev 26, 1398–1404.
[72] Thavaneswaran, S., Scammells, P.J., 2006. Further investigation of the N-demethylation of tertiary amine alkaloids using the non-classical Polonovski reaction. Bioorg Med Chem Lett 16, 2868–2871.
[73] Aleksandrov, Y.A., Sadikov, G.B., Tomadze, T.V., Golov, V.G., 1976. Nature of the primary products of the autoxidation and thermal polymerization of 4,4′-diisocyanatediphenylmethane. Khimiya Elementoorg Soedin 78–80.
[74] Aleksandrov, Y.A., Sadikov, G.B., Golov, V.G., 1978. Peroxide product of the autoxidation of 4,4′-diisocyanatodiphenylmethane. Zh Org Khimii 1873–1877.
[75] Wilhelm, C., Gardette, J.-L., 1997. Infrared analysis of the photochemical behaviour of segmented polyurethanes: 1. Aliphatic poly(ester-urethane). Polymer 38, 4019–4031.
[76] Wilhelm, C., Rivaton, A., Gardette, J.-L., 1998. Infrared analysis of the photochemical behaviour of segmented polyurethanes: 3. Aromatic diisocyanate based polymers. Polymer 39, 1223–1232.
[77] Servay, T., Voelkel, R., Schmiedberger, H., Lehmann, S., 2000. Thermal oxidation of the methylene diphenylene unit in MDI-TPU. Polymer 41, 5247–5256.
[78] Schultze, H., 1973. Über den photochemischen Abbau von Polyurethanen. Die Makromol Chem 172, 57–75.
[79] Malíková, M., Rychlý, J., Matisová-Rychlá, L., Csomorová, K., Janigová, I., Wilde, H.-W., 2010. Assessing the progress of degradation in polyurethanes by chemiluminescence. I. Unstabilised polyurethane films. Polym Degrad Stab 95, 2367–2375.
[80] Huang, T., Li, R., 2021. The effect of metal salts on polyurethane foam: antioxidation and reduction of VOCs emissions. J Polym Res 28.
[81] Goglev, R.S., Neiman, M.B., 1968. Thermal-oxidative degradation of the simpler polyalkyleneoxides. Polym Sci U S S R 9, 2351–2364.
[82] P. Grosborne, I. Sérée de Roch, L. Sajus, Bulletin de la Societé chimique de France 2020–2029.
[83] Erlandsson, B., 2002. Stability-indicating changes in poloxamers: the degradation of ethylene oxide-propylene oxide block copolymers at 25 and 40 °C. Polym Degrad Stab 78, 571–575.
[84] Santacesaria, E., Gelosa, D., Di Serio, M., Tesser, R., 1991. Thermal stability of nonionic polyoxyalkylene surfactants. J Appl Polym Sci 42, 2053–2061.
[85] Decker, C., 1977. Radiation-induced oxidation of solid poly(ethylene oxide). II. Mechanism. J Polym Sci Polym Chem Ed 15, 799–813.
[86] Griffiths, P.J., Hughes, J.G., Park, G.S., 1993. The autoxidation of poly(propylene oxide)s. Eur Polym J 29, 437–442.
[87] Gallet, G., Carroccio, S., Rizzarelli, P., Karlsson, S., 2002. Thermal degradation of poly(ethylene oxide–propylene oxide–ethylene oxide) triblock copolymer: comparative study by SEC/NMR, SEC/MALDI-TOF-MS and SPME/GC-MS. Polymer 43, 1081–1094.
[88] Yang, L., Heatley, F., Blease, T.G., Thompson, R.I., 1996. A study of the mechanism of the oxidative thermal degradation of poly(ethylene oxide) and poly (propylene oxide) using 1H- and 13C NMR. Eur Polym J 32, 535–547.
[89] Gauvin, P., Lemaire, J., Sallet, D., 1987. Photo-oxydation de polyéther-bloc-polyamides, 3†. Propriétés des hydroperoxydes dans les homopolym`res de polyéthers correspondants. Die Makromol Chem 188, 1815–1824.
[90] M. Ionescu, Chemistry and technology of polyols for polyurethanes, 2nd ed., A Smithers Group Company, Shawbury, Shrewsbury, Shropshire, 2016.
[91] Nash, T., 1953. The colorimetric estimation of formaldehyde by means of the Hantzsch reaction. Biochem J 55, 416–421.
[92] Verein Deutscher Ingenieure, Messen gasförmiger Emissionen: Messen aliphatischer Aldehyde (C1 bis C3) nach dem MBTH-Verfahren, Beuth Verlag GmbH, Düsseldorf, 1990.
[93] Verein Deutscher Ingenieure, Messen gasförmiger Emissionen: Messen von Formaldehyd nach dem AHMT-Verfahren, Beuth Verlag GmbH, Düsseldorf 13.040.20, 2001.
[94] Horning, E.C., Horning, M.G., 1946. Methone derivatives of aldehydes. J Org Chem 11, 95–99.
[95] Verein Deutscher Ingenieure, Messen von gasförmigen Immissionen: Messen von Innenraumluftverunreinigungen Messeen von Prüfgasen Bestimmung der Formaldehydkonzentration nach dem Sulfit-Pararosanilin-Verfahren, Beuth Verlag GmbH, Düsseldorf 13.040.20, 2001.
[96] Eegriwe, E., 1937. Reaktionen und Reagenzien zum Nachweis organischer Verbindungen IV). Fresenius, Z F Anal Chem 110, 22–25.
[97] Xie, C.J., Xie, P., Li, J., Yan, L.S., 2012. Pentafluorophenyl hydrazine as a derivatization agent for the determination of twenty carbonyl compounds in the atmosphere. AMR 610-613, 36–39.
[98] Ho, S.S.H., Yu, J.Z., 2004. Determination of airborne carbonyls: comparison of a thermal desorption/GC method with the standard DNPH/HPLC method. Environ Sci Technol 38, 862–870.
[99] Martos, P.A., Pawliszyn, J., 1998. Sampling and determination of formaldehyde using solid-phase microextraction with on-fiber derivatization. Anal Chem 70, 2311–2320.

[100] Bundesministerium für Umwelt Naturschutz und nukleare Sicherheit, Bekanntmachung analytischer Verfahren für Probennahmen und Untersuchungen für die in Anlage 1 der Chemikalien-Verbotsverordnung genannten Stoffe und Stoffgruppen. BAnz AT 26.11.2018 B2, Bundesanzeiger (2018).

[101] Böhm, M., Salem, M.Z.M., Srba, J., 2012. Formaldehyde emission monitoring from a variety of solid wood, plywood, blockboard and flooring products manufactured for building and furnishing materials. J Hazard Mater 221-222, 68–79.

[102] Kim, S., Kim, H.-J., 2005. Comparison of standard methods and gas chromatography method in determination of formaldehyde emission from MDF bonded with formaldehyde-based resins. Bioresour Technol 96, 1457–1464.

[103] Risholm-Sundman, M., Wallin, N., 1999. Comparison of different laboratory methods for determining the formaldehyde emission from three-layer parquet floors. Holz als Roh- und Werkst 57, 319–324.

[104] Risholm-Sundman, M., Larsen, A., Vestin, E., Weibull, A., 2007. Formaldehyde emission—comparison of different standard methods. Atmos Environ 41, 3193–3202.

[105] Verein Deutscher Ingenieure, Messen gasförmiger Emissionen: Messen alipatischer und aromatischer Aldehyde und Ketone nach dem DNPH-Verfahren Kartuschen Methode, Beuth Verlag GmbH, Düsseldorf 13.040.20, 2000.

[106] Verein Deutscher Ingenieure, Messen gasförmiger Emissionen: Messen aliphatischer und aromatischer Aldehyde und Ketone nach dem DNPH-Verfahren Gaswaschflaschen Methode, Beuth Verlag GmbH, Düsseldorf ICS 13.040.20, 2000.

[107] Epa (Ed.), Compendium of Methods for the Determination of Toxic Organic Compounds in Ambient Air: Determination of Formaldehyde in Ambient Air Using Adsorbent Cartridge Followed by High Performance Liquid Chromatography (HPLC). Active Sampling Methodology, Cincinnati, 1999.

[108] Deutsches Institut für Normung e.V, Innenraumluftverunreinigungen – Teil 4: Bestimmung von Formaldehyd – Probenahme mit Passivsammlern (ISO 16000–4: 2011), Beuth Verlag GmbH, Berlin 13.040.20, 2012.

[109] Deutsches Institut für Normung e.V, Innenraumluftverunreinigungen – Teil 3: Messen von Formaldehyd und anderen Carbonylverbindungen in der Innenraumluft und in Prüfkammern – Probenahme mit einer Pumpe (ISO 16000–3:2011), Beuth Verlag GmbH, Berlin 13.040.20, 2013.

[110] Schieweck, A., Uhde, E., Salthammer, T., 2021. Determination of acrolein in ambient air and in the atmosphere of environmental test chambers. Environ Sci Process Impacts 23, 1729–1746.

[111] Deutsches Institut für Normung e.V, Innenraumluftverunreinigungen – Teil 2: Probenahmestrategie für Formaldehyd (ISO 16000–2:2004); Deutsche Fassung EN ISO 16000–2:2006, Beuth Verlag GmbH, Berlin 13.040.20, 2006.

[112] Deutsches Institut für Normung e.V, Innenraumluftverunreinigungen – Teil 25: Bestimmung der Emission von schwerflüchtigen organischen Verbindungen aus Bauprodukten – Mikro-Prüfkammerverfahren (ISO 16000–25:2011), Beuth Verlag GmbH, Berlin 13.040.20, 2012.

[113] Verband der Automobilindustrie, Formteile für den Fahrzeuginnenraum Bestimmung der Formaldehydabgabe Meßverfahren nach der modifizierten Flaschen-Methode, 1994.

[114] Verband der Automobilindustrie, Nichtmetallische Werkstoffe der Kfz-Innenausstattung Bestimmung der Emission organischer Verbindungen, 1995.

[115] Verband der Automobilindustrie, Thermodesorptionsanalyse organischer Emissionen zur Charakterisierung von nichtmetallischen KFZ-Werkstoffen, 2002.

[116] Huang, S., Xiong, J., Cai, C., Xu, W., Zhang, Y., 2016. Influence of humidity on the initial emittable concentration of formaldehyde and hexaldehyde in building materials: experimental observation and correlation. Sci Rep 6, 23388.

[117] Kang, Y., Yoo, S.-J., Ito, K., 2021. Correlation between formaldehyde emission characteristics in enclosed desiccators with five different geometries. Indoor Built Environ 30, 565–577.

[118] Kang, Y., Yoo, S.-J., Takenouchi, K., Yoshida, H., Tanabe, S., Ito, K., 2019. Distribution of transient formaldehyde concentration in confined small glass desiccators and its impact on emission rate measurement. Atmos Environ 218, 116979.

[119] Salem, M.Z.M., Böhm, M., Barcík, Š., Beránková, J., 2011. Formaldehyde emission from wood-based panels bonded with different formaldehyde-based resins. Drv Ind 62, 177–183.

[120] Hemmilä, V., Meyer, B., Larsen, A., Schwab, H., Adamopoulos, S., 2019. Influencing factors, repeatability and correlation of chamber methods in measuring formaldehyde emissions from fiber- and particleboards. Int J Adhes Adhes 95, 102420.

[121] Yu, C., Crump, D.R., 1999. Testing for formaldehyde emission from wood-based products – a review. Indoor Built Environ 8, 280–286.

[122] Salem, M.Z.M., Böhm, M., Barcík, Š., Srba, J., 2012. Inter-laboratory comparison of formaldehyde emission from particleboard using ASTM D 6007-02 method. Holz als Roh- und Werkst 70, 621–628.

[123] Zhang, Y., Luo, X., Wang, X., Qian, K., Zhao, R., 2007. Influence of temperature on formaldehyde emission parameters of dry building materials. Atmos Environ 41, 3203–3216.

[124] Wang, X., Zhang, Y., 2009. A new method for determining the initial mobile formaldehyde concentrations, partition coefficients, and diffusion coefficients of dry building materials. J Air Waste Manag Assoc (1995) 59, 819–825.

[125] Cox, S.S., Zhao, D., Little, J.C., 2001. Measuring partition and diffusion coefficients for volatile organic compounds in vinyl flooring. Atmos Environ 35, 3823–3830.

[126] Ye, W., Cox, S.S., Zhao, X., Frazier, C.E., Little, J.C., 2014. Partially-irreversible sorption of formaldehyde in five polymers. Atmos Environ 99, 288–297.

[127] Cox, S.S., Little, J.C., Hodgson, A.T., 2001. Measuring concentrations of volatile organic compounds in vinyl flooring. J Air Waste Manag Assoc (1995) 51, 1195–1201.

[128] Smith, J.F., Gao, Z., Zhang, J.S., Guo, B., 2009. A new experimental method for the determination of emittable initial VOC concentrations in building materials and sorption isotherms for IVOCs. Clean Soil Air Water 37, 454–458.

[129] Xiong, J., Zhang, Y., 2010. Impact of temperature on the initial emittable concentration of formaldehyde in building materials: experimental observation. Indoor Air 20, 523–529.

[130] Xiong, J., Chen, W., Smith, J.F., Zhang, Y., Zhang, J.S., 2009. An improved extraction method to determine the initial emittable concentration and the partition coefficient of VOCs in dry building materials. Atmos Environ 43, 4102–4107.

[131] Xiong, J., Yan, W., Zhang, Y., 2011. Variable volume loading method: a convenient and rapid method for measuring the initial emittable concentration and partition coefficient of formaldehyde and other aldehydes in building materials. Environ Sci Technol 45, 10111–10116.

[132] Xiong, J., Yao, Y., Zhang, Y., 2011. C-history method: rapid measurement of the initial emittable concentration, diffusion and partition coefficients for formaldehyde and VOCs in building materials. Environ Sci Technol 45, 3584–3590.

[133] Deutsches Institut für Normung e.V, DIN ISO 12219–1 Innenraumluft von Straßenfahrzeugen: Teil 1 Gesamtfahrzeugprüfkammer Spezifikation und Verfahren zur Bestimmung von flüchtigen organischen Verbindungen in Fahrzeugkabinen, Beuth Verlag GmbH, Berlin 13.040.20; 43.020, 2022.

[134] D. Poppendieck, M. Gong, L. Lawson, Lessons learned from spray polyurethane foam emission testing using micro-chambers, 2016.

[135] D. Poppendieck, M. Gong, S. Emmerich, Characterization of emissions from spray polyurethane foam - final report to U.S. Consumer Product Safety Commission, National Institute of Standards and Technology, Gaithersburg, MD, 2017.

[136] Bidleman, T.F., Tysklind, M., 2018. Breakthrough during air sampling with polyurethane foam: What do PUF 2/PUF 1 ratios mean? Chemosphere 192, 267–271.

[137] Billings, W.N., Bidleman, T.F., 1980. Field comparison of polyurethane foam and Tenax-GC resin for high-volume air sampling of chlorinated hydrocarbons. Environ Sci Technol 14, 679–683.

[138] Brenner, K.S., Dorn, I.H., Menz, G., 1994. Polyurethane (PU)-foam-plug/impinger sampling train for monitoring of PCDD/F-emissions from incinerators and other emission sources. Toxicol Environ Chem 41, 187–207.

[139] Burdick, N.F., Bidleman, T.F., 1981. Frontal movement of hexachlorobenzene and polychlorinated biphenyl vapors through polyurethane. Anal Chem 53, 1926–1929.

[140] Chaemfa, C., Wild, E., Davison, B., Barber, J.L., Jones, K.C., 2009. A study of aerosol entrapment and the influence of wind speed, chamber design and foam density on polyurethane foam passive air samplers used for persistent organic pollutants. J Environ Monit 11, 1135–1139.

[141] Bidleman, T.F., Simon, C.G., Burdick, N.F., You, F., 1984. Theoretical plate measurements and collection efficiencies for high-volume air samplers using polyurethane foam. J Chromatogr A 301, 448–453.

[142] Kamprad, I., Goss, K.-U., 2007. Systematic investigation of the sorption properties of polyurethane foams for organic vapors. Anal Chem 79, 4222–4227.

[143] Ligocki, M.P., Pankow, J.F., 1985. Assessment of adsorption/solvent extraction with polyurethane foam and adsorption/thermal desorption with Tenax-GC for the collection and analysis of ambient organic vapors. Anal Chem 57, 1138–1144.

[144] Pankow, J.F., 1989. Overview of the gas phase retention volume behavior of organic compounds on polyurethane foam. Atmos Environ (1967) 23, 1107–1111.

[145] Strandberg, B., Julander, A., Sjöström, M., Lewné, M., Koca Akdeva, H., Bigert, C., 2018. Evaluation of polyurethane foam passive air sampler (PUF) as a tool for occupational PAH measurements. Chemosphere 190, 35–42.

[146] Tromp, P.C., Beeltje, H., Okeme, J.O., Vermeulen, R., Pronk, A., Diamond, M.L., 2019. Calibration of polydimethylsiloxane and polyurethane foam passive air samplers for measuring semi volatile organic compounds using a novel exposure chamber design. Chemosphere 227, 435–443.

[147] Kim, K., Shin, H.-M., Wong, L., Young, T.M., Bennett, D.H., 2021. Evaluating couch polyurethane foam for a potential passive sampler of semivolatile organic compounds. Chemosphere 271, 129349.

[148] He, J.-J., Jiang, L., Sun, J.-H., Lo, S., 2016. Thermal degradation study of pure rigid polyurethane in oxidative and non-oxidative atmospheres. J Anal Appl Pyrolysis 120, 269–283.

[149] Jiao, L., Xiao, H., Wang, Q., Sun, J.-H., 2013. Thermal degradation characteristics of rigid polyurethane foam and the volatile products analysis with TG-FTIR-MS. Polym Degrad Stab 98, 2687–2696.

[150] Herrera, M., Matuschek, G., Kettrup, A., 2002. Thermal degradation of thermoplastic polyurethane elastomers (TPU) based on MDI. Polym Degrad Stab 78, 323–331.

[151] Jellinek, H.H.G., Takada, K., 1975. Toxic gas evolution from polymers: evolution of hydrogen cyanide from linear polyurethane. J Polym Sci Polym Chem Ed 13, 2709–2723.

[152] Jellinek, H.H.G., Dunkle, S.R., 1983. Kinetics and mechanism of HCN-evolution from the oxidation of polyurethanes. J Polym Sci Polym Chem Ed 21, 487–511.

[153] E. Fitzer, W. Fritz, G. Emig, Technische Chemie: Einführung in die Chemische Reaktionstechnik, Springer Berlin Heidelberg, Berlin, Heidelberg, 1995.

[154] D.A. Crowl, J.F. Louvar, Chemical process safety: Fundamentals with applications, Prentice-Hall, Englewood Cliffs, New Jersey, op. 2011.

[155] Herrington, J.S., Fan, Z.-H.T., Lioy, P.J., Zhang, J.J., 2007. Low acetaldehyde collection efficiencies for 24-hour sampling with 2,4-dinitrophenylhydrazine (DNPH)-coated solid sorbents. Environ Sci Technol 41, 580–585.
[156] Herrington, J.S., Hays, M.D., 2012. Concerns regarding 24-h sampling for formaldehyde, acetaldehyde, and acrolein using 2,4-dinitrophenylhydrazine (DNPH)-coated solid sorbents. Atmos Environ 55, 179–184.
[157] Ho, S.S.H., Ho, K.F., Liu, W.D., Lee, S.C., Dai, W.T., Cao, J.J., Ip, H., 2011. Unsuitability of using the DNPH-coated solid sorbent cartridge for determination of airborne unsaturated carbonyls. Atmos Environ 45, 261–265.
[158] ASTM International, D5197–09e1: Standard Test Method for Determination of Formaldehyde and Other Carbonyl Compounds in Air (Active Sampler Methodology).
[159] ASTM International, D5197–21: Designation: D5197 − 21 Standard Test Method for Determination of Formaldehyde and Other Carbonyl Compounds in Air (Active Sampler Methodology).
[160] Schulte-Ladbeck, R., Lindahl, R., Levin, J.O., Karst, U., 2001. Characterization of chemical interferences in the determination of unsaturated aldehydes using aromatic hydrazine reagents and liquid chromatography. J Environ Monit JEM 3, 306–310.
[161] Audouin, L., Langlois, V., Verdu, J., de Bruijn, J.C.M., 1994. Role of oxygen diffusion in polymer ageing: kinetic and mechanical aspects. J Mater Sci 29, 569–583.
[162] Celina, M.C., Gillen, K.T., 2005. Oxygen permeability measurements on elastomers at temperatures up to 225 °C. Macromolecules 38, 2754–2763.
[163] Hennebert, P., 1988. Solubility and diffusion coefficients of gaseous formaldehyde in polymers. Biomaterials 9, 162–167.
[164] de Sainte Claire, P., 2009. Degradation of PEO in the solid state: a theoretical kinetic model. Macromolecules 42, 3469–3482.
[165] Vanos, J.K., Middel, A., Poletti, M.N., Selover, N.J., 2018. Evaluating the impact of solar radiation on pediatric heat balance within enclosed, hot vehicles. Temp (Austin, Tex) 5, 276–292.
[166] Fruin, S.A., Hudda, N., Sioutas, C., Delfino, R.J., 2011. Predictive model for vehicle air exchange rates based on a large, representative sample. Environ Sci Technol 45, 3569–3575.
[167] Jankowski, Indoor air guide values derived by the German Committee on Indoor Air Guide Values (AIR) 2023.
[168] European Commission, Agreed EU-LCI values (December 2022) (2022).
[169] Ministry of Environmental Protection of the People's Republic of China, Guideline for air quality assessment of passenger car, Standardization Administration of the People's Republic of China (SAC), CN 13.040.30; 13.040.40, 2012.
[170] Ministry of Land, Infrastructure and Transport, The Management Standards of the Interior Air Quality of Newly Manufactured Vehicles, Korea, 2013, ⟨https://wiki.unece.org/download/attachments/29229239/VIAQ-03–08%20-%20Korea_VIAQ_Standards.doc?api=v2⟩, accessed 1 September 2023.
[171] Feron, V.J., Kruysse, A., Til, H.P., Immel, H.R., 1978. Repeated exposure to acrolein vapour: subacute studies in hamsters, rats and rabbits. Toxicology 9, 47–57.
[172] Ruth, J.H., 1986. Odor thresholds and irritation levels of several chemical substances: a review. Am Ind Hyg Assoc J 47. A142-51.
[173] NAC/AEGL FACA Committee, INTERIM ACUTE EXPOSURE GUIDELINE LEVELS (AEGLs) FOR FORMALDEHYDE: (CAS Reg. No. 50–00-0) (2008).
[174] NAC/AEGL FACA Committee, Acetaldehyde Interim AEGL Document 2009 (2009).
[175] National Research Council (U.S.), Acute exposure guideline levels for selected airborne chemicals, National Academy Press, Washington D.C., 2000-<2016>.
[176] Yoshida, T., Matsunaga, I., Tomioka, K., Kumagai, S., 2006. Interior air pollution in automotive cabins by volatile organic compounds diffusing from interior materials: I. Survey of 101 types of japanese domestically produced cars for private use. Indoor Built Environ 15, 425–444.
[177] Mikheyev, Y., Guseva, L.N., Mikheyeva, L., Toptygin, D., 1989. The chain degradation of polyethylene oxide and polypropylene hydroperoxides. Polym Sci U S S R 31, 1094–1101.
[178] Al-Rawashdeh, H., Hasan, A.O., Al-Shakhanbeh, H.A., Al-Dhaifallah, M., Gomaa, M.R., Rezk, H., 2021. Investigation of the effect of solar ventilation on the cabin temperature of vehicles parked under the sun. Sustainability 13, 13963.
[179] Huang, S., Xiong, J., Zhang, Y., 2015. The impact of relative humidity on the emission behaviour of formaldehyde in building materials. Procedia Eng 121, 59–66.
[180] Europur, REACH Restriction on Formaldehyde Released from Articles (2023).